

SEQUENCE STRATIGRAPHY OF THE BARNETT SHALE  
(MISSISSIPPIAN), NORTHERN FORT WORTH BASIN, TEXAS

By

MICHAEL BAILEY STEED

Bachelor of Science, 2006  
Texas Christian University  
Fort Worth, Texas

Submitted to the Graduate Faculty of  
The College of Science and Engineering  
Texas Christian University  
In partial fulfillment of the requirements for the degree of

MASTER OF SCIENCE

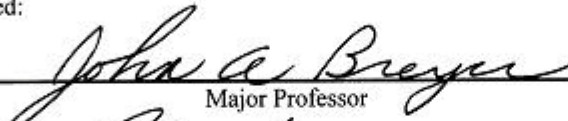
May 2009

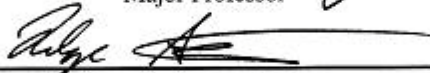
SEQUENCE STRATIGRAPHY OF THE BARNETT SHALE  
(MISSISSIPPIAN), NORTHERN FORT WORTH BASIN, TEXAS

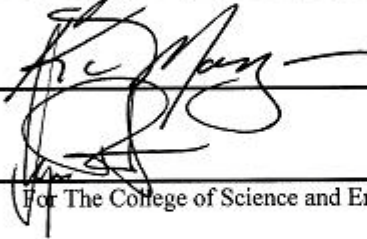
by

Michael Bailey Steed

Dissertation approved:

  
Major Professor



  
For The College of Science and Engineering

Copyright by  
Michael B. Steed  
2009

## **Acknowledgments**

I gratefully acknowledge all those who provided assistance, advice, resources, and guidance during the compilation of this thesis. Without their generosity this project would have been impossible. The time spent studying the Barnett Shale has acquainted me with a subject of great interest to the Fort Worth community. The Barnett Shale, and more importantly, the oil & gas industry is where I plan to pursue a career. Experience from this project has provided me a foundation to achieve that goal in the future.

I thank everyone at IHS who helped during the study. They helped answer questions that seemed impossible. I would also like to show my most sincere gratitude to the TCU Energy Institute for providing financial support that aided in obtaining the log images for this project. Most importantly I would like to thank Dr. John Breyer for his guidance and patience throughout the study.

## Table of Contents

Acknowledgments.....	ii
List of Figures.....	iv
Introduction.....	1
Geographic and Geologic Setting.....	3
Previous Work.....	7
Sequence Stratigraphy in Shale-Rich Basins.....	9
Methodology/Justification.....	13
Study Area and Procedure.....	15
Results.....	18
Discussion.....	42
Conclusions.....	44
References.....	46
Appendices.....	51
Appendix I.....	51
Appendix II.....	55
Appendix III.....	61
Vita	
Abstract	

## List of Figures

1.	Sea level curve for the Mississippian.....	2
2.	Map of Fort Worth basin.....	4
3.	Stratigraphic column.....	5
4.	Map of study area.....	16
5.	Type logs from Mitchell Energy William Tedrow Gas #4.....	17
6.	Structure map on the base of the Barnett Shale.....	20
7.	Structure map on GRS-1.....	22
8.	Structure map on GRS-2.....	23
9.	Structure map on GRS-3.....	24
10.	Structure map on GRS-4.....	25
11.	Structure map on GRS-5.....	26
12.	Structure map on GRS-6.....	27
13.	Structure map on top of Forestburg limestone.....	29
14.	Structure map on top of Forestburg shale.....	30
15.	Isopach map base of Barnett to GRS-1.....	32
16.	Isopach map GRS-1 to GRS-2.....	33
17.	Isopach map GRS-2 to GRS-3.....	34
18.	Isopach map GRS-3 to GRS-4.....	35
19.	Isopach map GRS-4 to GRS-5.....	37
20.	Isopach map GRS-5 to GRS-6.....	38
21.	Isopach map of Forestburg limestone.....	39

## INTRODUCTION

The Barnett Shale (Mississippian) in north-central Texas is a world-class unconventional oil and gas reservoir deposited in a deepwater environment over a period of 25 million years, from 345 to 320 million years ago (Montgomery et al., 2005; Loucks and Ruppel, 2007). Except for a small area in the northern Fort Worth basin, where Henry (1982) recognized five distinct members, the Barnett Shale has not been subdivided into smaller units for stratigraphic analysis. The purpose of this study is to develop a detailed sequence stratigraphic framework for the Barnett. Deposition of the Barnett took place during a prolonged second-order highstand of global sea level. At least ten third-order cycles of change in global sea level took place during this second-order highstand (Ross and Ross, 1988). Third-order cycles of relative change in sea level produce the depositional sequences of seismic and sequence stratigraphy (Vail et al., 1977, 1991). The depositional sequences formed during third-order cycles of sea level change in the Mississippian provide a basis for subdividing the Barnett Shale for more detailed stratigraphic analysis (Fig. 1).

Recent work suggests patterns on gamma-ray logs can be used to recognize maximum flooding surfaces, parasequences and parasequence sets in shale basins (Bohacs, 1998; Creaney and Passey, 1993). Parasequences and parasequence sets are the building blocks of the systems tracts recognized in sequence stratigraphy (Van Wagoner et al., 1988; Van Wagoner et al., 1990). Distinctive stacking patterns can be used to assign parasequence sets to highstand, lowstand or transgressive systems tracts (see below). I will use these stacking patterns and maximum flooding surfaces to subdivide the Barnett Shale in the Fort Worth into systems tracts and depositional sequences.

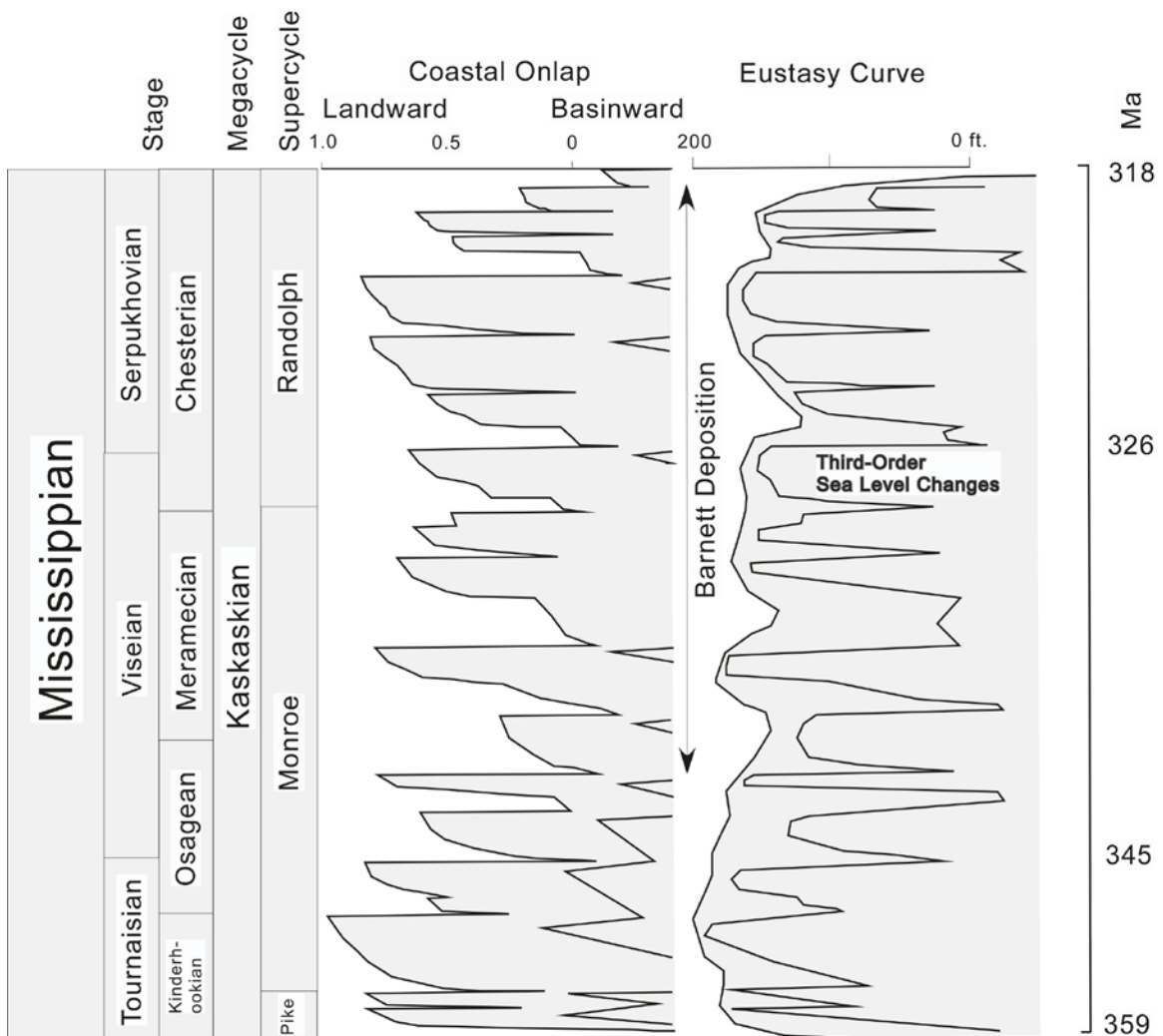


**Figure 1.** Coastal onlap and eustasy curves for the Mississippian. Modified slightly from Loucks and Ruppel (2007). Curves modified from Ross and Ross (1987).



## **GEOGRAPHIC AND GEOLOGIC SETTING**

The Fort Worth basin extends some 200 to 250 miles from the Red River arch in the north to the Llano uplift in the south (Fig. 2). It has a maximum width of about 125 miles on a line that runs across the top of Palo Pinto, Parker, Tarrant and Dallas counties, approximately at the latitude of the city of Dallas. The Bend arch forms the western margin of the basin and the Ouachita thrust front forms the eastern margin. The basin covers approximately 15,000 square miles. It is one of a series of foreland basins formed along the southern margin of the North American craton during the late Paleozoic Ouachita orogeny. Other basins formed at this time include the Black Warrior basin to the east and the Kerr, Val Verde and Marfa basins to the west (Flawn et al., 1961; Walper, 1982).

Paleozoic strata comprise almost the entire fill of the Fort Worth basin (Fig. 3). The basin contains 4,000 to 5,000 feet of Ordovician through Mississippian limestone, dolomite and shale, and 6,000 to 7,000 feet of Pennsylvanian clastics overlain by a thin wedge of Cretaceous strata (Montgomery et al., 2005). The basin fill thickens to the northeast, into the Oklahoma aulcogen, and thins to the south and west, toward the Llano uplift and the Bend arch, respectively. Over 12,000 feet of sediment is present immediately adjacent the Muenster arch—a fault block bound by basement faults reactivated during the late Paleozoic. Here the top of the Ellenburger Group, which immediately underlies the Barnett Shale over much of the basin, is found at a depth of 8,000 to 9,000 feet. The top of the Ellenburger ascends to the surface to the southwest around the flanks of the Llano uplift. The Barnett is also thickest (700 to 1,000 feet) to

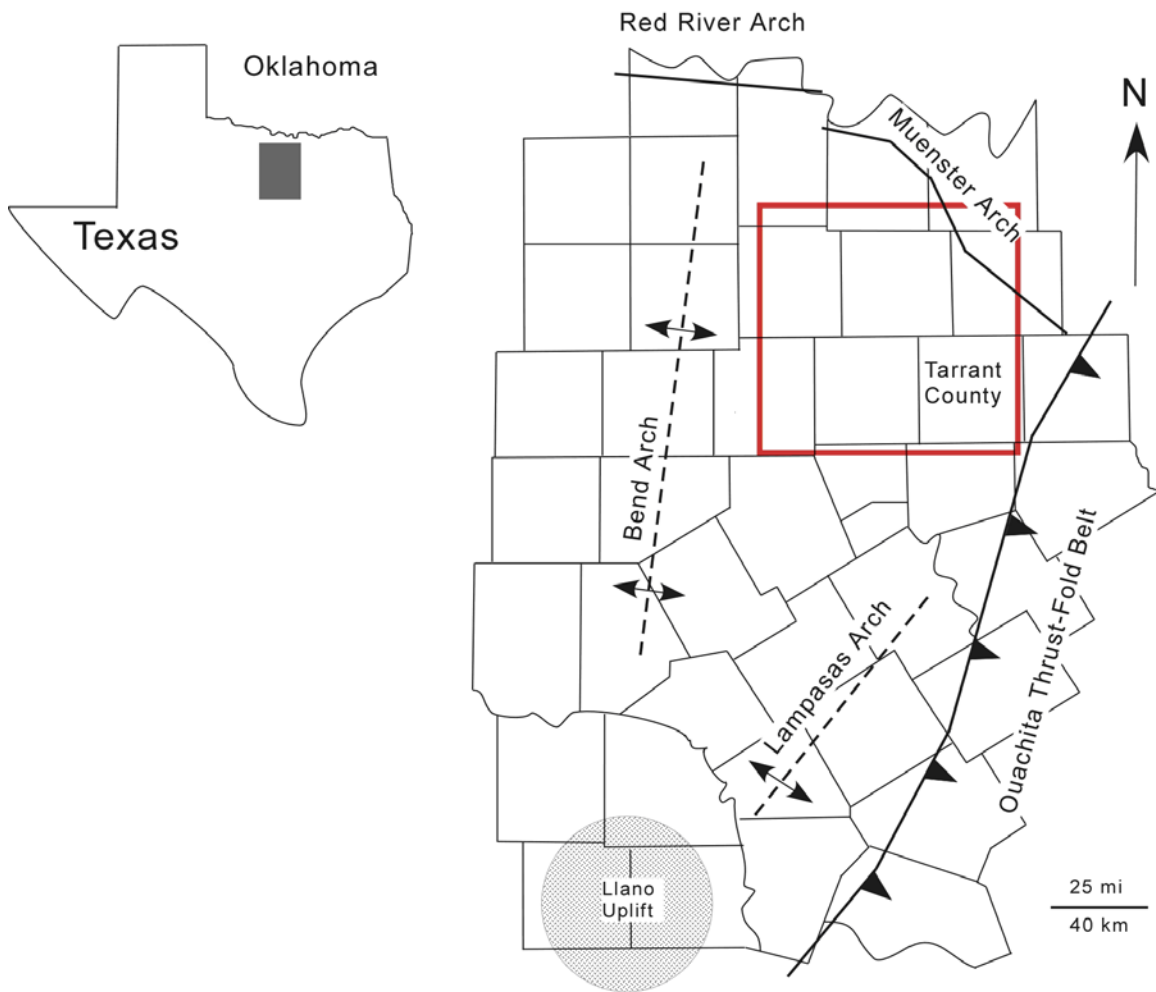


**Figure 2.** Map of the Fort Worth basin showing bounding geologic features. Red box shows location of the study area.

System	Series	Group or Formation
Cretaceous	Comanchean	Trinity Group
	Unconformity	
Pennsylvanian	Virgilian	Strawn Group
	Missourian	Bend Group
	Desmoinesian	
	Atokan	
	Morrowan	
Mississippian	Chesterian	Barnett Shale
	Meramecian	
	Osagean	
	Kinderhookian	
Unconformity		
Ordovician	Upper	Viola Group
	Lower	Simpson Group Ellenburger Group
Cambrian	Upper	Wilberns-Riley
Precambrian		

**Figure 3.** Stratigraphic column for the Fort Worth basin. After Montgomery et al. (2005).

the northeast against the Muenster arch and thins to a feather edge (<30 feet) over the Llano uplift to the southwest. The Barnett also thins to the west over the Bend arch where it interfingers of the Chappel Formation (Henry, 1982; Flippin, 1982; Kier et al., 1980; Mapel et al., 1979).

Following an extensive early Paleozoic transgression, erosion removed all of the Silurian and Devonian strata from the Fort Worth basin (Henry, 1982). The Barnett was the first unit to be deposited when the seas returned. The shale was deposited on a karsted surface. It developed on the top of the Ellenburger Group over a wide area (Kier et al., 1980). A subtle angular unconformity (<1°) is present between the Barnett Shale and the underlying limestones of the Ellenburger Group (Henry, 1982). An unconformity also separates the Barnett from the overlying Pennsylvanian strata (Cheney, 1940). Older stratigraphic studies suggest that most of the Barnett accumulated either on a normal marine shelf (Henry, 1982) or in a relatively shallow, starved basin under euxinic conditions (Kier et al., 1980). However, more recent work interprets the Barnett Shale in the Fort Worth basin as deep-water slope-to-basin deposit. Loucks and Ruppel (2007) estimated water depths from 400 feet to 700 feet during the deposition of the Barnett. Bottom waters were dysaerobic to anaerobic allowing organic matter in the shale to be preserved.

Plate and paleogeographic reconstructions by Blakey (2005) show the area of the Fort Worth basin covered by relatively deep waters during the Late Mississippian. Water depths become shallower to the west (present day directions) toward the Chappel shelf and Llano uplift where exposed areas served as sources of terrigenous sediment. To the south and east was an arc-trench system formed by the subduction of the North American

plate beneath the South American plate. Laurussia to the north and Gondwana to the south were being brought together as the ocean between them closed.

## **PREVIOUS WORK**

The Barnett Shale was named by F. B. Plummer and R. C. Moore in a University of Texas Bulletin published in 1922. The type section is an outcrop in San Saba County. Until recently, the Barnett was known almost exclusively from the study of outcrops in central Texas on the Llano uplift. The formation has received little attention in studies of the geology of the Fort Worth basin. Although the Barnett Shale has recently attracted considerable attention from petroleum geologists only a small number of detailed sedimentological and/or petrographic studies are available in the public domain.

Cheney (1940) showed the Barnett on several cross sections in his study of the Paleozoic strata in the subsurface of north-central Texas. His Figure 9 showed a structure contour map drawn on the base of the Barnett (top of the Ellenburger), but otherwise provided little information on the formation. Henry (1982) noted subsurface studies of the Barnett Shale and its lateral equivalent the Chappel Formation were but “modestly represented in the literature.” He noted that the Barnett had a distinctive signature on resistivity and gamma-ray logs. He then subdivided the Barnett Shale in Jack County into five informal members using well log criteria. The members could not be traced northward much beyond the southwestern portion of Montague County because the distinctive log patterns disappeared. Lack of well control prevented Henry (1982) from tracing his informal members eastward into the Fort Worth basin in Wise County. He did

observe, however, that calcareous shale appeared in the Barnett in southeastern Montague County and that the section became progressively limier toward the east and north.

In the northeastern part of the Fort Worth basin, where the Barnett is thickest, it contains significant amounts of limestone (Montgomery et al., 2005). In Newark East Field and the surrounding areas in Wise, Denton and northern Tarrant counties the Barnett is divided into an upper and lower member by the Forestburg limestone. Beyond the limits of the Forestburg, throughout most of the basin, the Barnett Shale is undifferentiated into smaller units.

Papazis (2005) provided a detailed petrographic characterization of samples of the Barnett Shale from core from four wells and four outcrops. The core came from wells in the northern and west-central portions of the basin. He utilized polarized light microscopy, secondary and back-scattered electron imaging, cathodoluminescence imaging, x-ray mapping and x-ray diffraction to characterize five major lithologic groups identified in core. He concluded that the Barnett was deposited in a relatively shallow epicontinental sea. Hickey and Henk (2007) recognized six lithofacies in a study of core from the Mitchell 2 T. P. Sims well in Newark East Field in Wise County in the northern portion of the basin. They interpret the facies as basinal deposits that include shallow-water components resedimented from slope settings. Bunting (2007) described a 200-foot core of Barnett Shale taken from a well in western Johnson County in the southeastern part of the Fort Worth Basin. He presented point counts and Rock-Eval pyrolysis data on a foot-by-foot basis over the entire length of core. He concluded that energy levels fluctuated during the deposition of the Barnett, but did not speculate at the specific environment of deposition.

Loucks and Ruppel (2007) devised a generalized depositional model for the Barnett showing the depositional processes and a depositional profile from the shelf into the basin. Major depositional processes include suspension settling from hemipelagic mud plumes, rapid deposition from turbidity currents and debris flows, and a constant settling of microscopic pelagic organisms, including both foraminifera and radiolarians. Phosphate minerals were precipitated on the upper part of the slope and framboidal pyrite formed in the water column below the oxygen minimum layer. The bottom waters and the sediments below them were dysaerobic to anaerobic, allowing abundant organic matter to be preserved. Contour currents flowed along the base of the slope and reworked the sediment there.

### **SEQUENCE STRATIGRAPHY IN SHALE-RICH BASINS**

Sequence stratigraphy provides a means of partitioning the fill of a sedimentary basin into smaller units for analysis. It is a type of allostratigraphy as redefined by Walker (1992). The depositional sequence is the fundamental unit of sequence stratigraphy. A depositional sequence is “a stratigraphic unit composed of a relatively conformable succession of genetically related strata and bounded at its top and base by unconformities or their correlative conformities.” (Mitchum et al., 1977). Sequences are produced by third-order cycles of relative change in sea level (Vail et al., 1977) and sequence-bounding unconformities form as a result of forced regressions caused by eustasy, tectonism or some combination of the two (Posamentier and Allen, 1999).

Sequences can be subdivided into systems tracts. Systems tracts are defined by their bounding surfaces, their position within a sequence, and by parasequence stacking

patterns (Van Wagoner et al., 1988). Three systems tracts are generally recognized: the highstand systems tract (HST), the lowstand systems tract (LST) and the transgressive systems tract (TST). The TST is bound by the transgressive surface below and the maximum flooding surface (condensed section) above. The HST lies on the maximum flooding surface and is overlain by the unconformity that forms the sequence boundary. The LST lies on the erosional surface associated with the sequence-bounding unconformity or its correlative conformity. It is overlain by the transgressive surface. Parasequences and parasequence sets are the building blocks of systems tracts and of depositional sequences. A parasequence is a “relatively conformable succession of genetically related beds or bedsets bounded by marine flooding surfaces or their correlative surfaces.” (Van Wagoner et al., (1990). Parasequences are generally taken to represent fourth-order cycles of relative change in sea level. The concept of parasequences was developed for sediments in shallow marine settings, but has been applied to other depositional settings as well, including deep-water environments, although Posamentier and Allen (1999) question this practice.

In shallow marine siliciclastic settings, parasequences are small scale, shoaling and coarsening upward units formed by either progradation or aggradation of the shoreline (Van Wagoner et al., 1990). These coarsening-upward units are easily recognized in the subsurface on logs (gamma ray and SP) that respond primarily to changes in grain size. In many cases systems tracts display characteristic parasequence stacking patterns. Three types of parasequence stacking patterns are recognized—progradational, aggradational and retrogradational (Van Wagoner et al., 1990). The



transgressive system tract shows a retrogradational stacking pattern and the late highstand systems tract shows a progradational stacking pattern.

At some point seaward of the coastline, the sequence-bounding unconformity dies out and passes basinward into its correlative conformity. Sedimentation is continuous across this surface and no hiatus occurs. In basinal settings, where sedimentation is continuous, the correlative conformity will be in a continuous sequence of pelagic and hemipelagic sediment. Such a surface would be impossible to recognize by lithologic criteria in outcrop or core. No physical basis for a distinctive log signature would exist. Surfaces other than correlative conformities must be used if the concepts of sequence stratigraphy are to be applied to thick shale sequences that accumulated in deep-water settings. The maximum flooding surface that forms the boundary between the TST and the HST is such a surface. A distinctive “condensed section” characterized by abundant biogenic and chemogenic sediment will form in the basin during the maximum flooding of the shelf when most terrigenous sediment is trapped in estuaries and bays high on paleoslope (Loutit et al., 1988).

Creaney and Passey (1993) and Bohacs (1998) have suggested ways in which sequence stratigraphy can be applied to basinal shale sequences using well logs. Their methods assume that the total organic carbon (TOC) content of the shale can be read either directly from spectral gamma ray logs or from combinations of sonic and resistivity logs. Using these assumptions both authors are able to recognize distinctive parasequence stacking patterns related to specific systems tracts, and also the maximum flooding surface between the TST and HST. The justification for using these assumptions about the TOC content of the shale is discussed below.

Creaney and Passey (1993) explain recurrent patterns in the vertical distribution of TOC in marine source rocks using sequence stratigraphic concepts. They assume that in dysaerobic or anaerobic basinal settings the TOC content of shale varies inversely with the influx of terrigenous clastic sediment. Given these assumptions, the highest TOC content in a shale sequence will be at the maximum flooding surfaces (condensed section) and the organic material will be increasingly oil prone. Creaney and Passey (1993) use overlays of sonic and resistivity logs to define packages of shale with sharp bases and high TOC toward the base (HTB units). These can occur as isolated packages of sediment but most commonly are found in stacks of several HTB units. Variation in the TOC content of the HTB units can be related to the influx of terrigenous sediment from the basin margin and interpreted in terms of parasequence stacking patterns and systems tracts (Creaney and Passey, 1993, their Figures 7 and 9). The characteristic stacking patterns are best expressed within the basin in distal rather than proximal settings.

Bohacs (1998) also presents a method of doing sequence stratigraphy in shale-rich basins. He provides criteria for recognizing sequence boundaries and flooding surfaces in both basinal and shelfal marine environments. Lithofacies characterized by different types and amounts of organic matter form at different places within a basin. The TOC content of the shale can be inferred from levels of uranium recorded on spectral gamma ray logs.

High levels of uranium correlate with high levels of organic matter and chemogenic sediments, notably phosphatic material, found in the condensed intervals associated with marine flooding surfaces (see below). The highest levels of uranium will

mark the time of maximum flooding of the shelf. Variations in TOC recognized on spectral gamma ray logs can be interpreted in terms of parasequence stacking patterns and systems tracts as with the method of Creaney and Passey (1993).

## **METHODOLOGY/JUSTIFICATION**

I could not use the method of Creaney and Passey (1993) based on the stacking patterns of HTB units because the porosity logs needed to calculate TOC were not available from a large enough sample of wells. Instead I obtained raster images of gamma ray logs from 131 wells in the Fort Worth Basin. Spectral gamma ray logs were available for only a few wells. High gamma ray counts (>150 API units) in the Barnett on these logs coincided with a high uranium content (10-30 ppm). Pennsylvanian shale above the Barnett had gamma ray readings of 120 API units and uranium concentrations of 2 to 4 ppm.

Based on these few wells, I assumed that high gamma ray readings in the Barnett resulted from an increase in uranium and that this resulted from enrichment associated with the presence of either organic or phosphatic material or both (see discussion below). Organic material, phosphatized grains and phosphatic nodules are often concentrated in condensed sections associated with flooding surfaces (Loutit et al., 1988). The highest concentrations of these materials are typically associated with the maximum flooding surface separating the TST from the HST.

### **TOC from Gamma Ray Logs**

Beers (1945) demonstrated a correlation between the uranium content and carbon content of black shales in the Paleozoic strata of the Michigan basin. A correlation

between uranium concentration and TOC content has been noted by other workers as well. Schmoker (1981) devised an equation for calculating the organic matter content of Devonian black shales in the western part of the Appalachian basin from gamma ray intensity measured in API units. He found that shale facies rich in organic matter had high gamma ray counts, and furthermore, that this was due mainly to an increase in uranium concentration. Concentrations of potassium-40 and thorium remained relatively constant throughout the entire shale section at any given locality, but the concentration of uranium varied directly with the organic matter content of the shale. Schmoker (1981) concluded that visual inspection of gamma ray logs was adequate for obtaining qualitative estimates of the relative concentration of organic matter in shale.

Supernaw et al. (1978) in claims in a patent application asserted that spectral gamma ray logs could be used to determine the source rock potential of formations encountered in a borehole. The uranium concentration of the New Albany Shale had a correlation coefficient of 0.977 with the TOC content (Supernaw et al., 1978, their Figure 3). The correlation is explained by the electrical affinity between uranium salts dissolved in seawater and organic carbon in bottom sediments. Uranium from seawater and pore fluids is also concentrated in phosphatic material (Baturin, 1982).

Passey et al. (1990) presented a popular model for determining organic richness (TOC) of potential source rocks using gamma ray, porosity and resistivity logs. Any of the three common porosity logs (sonic, neutron or density) can be used, but the sonic log is preferred. The gamma ray log is used to eliminate reservoir rocks from the analysis, but is not used in calculating the TOC content of potential source rocks.

## **STUDY AREA AND PROCEDURE**

The study area includes eight counties in the northern and central portions of the Fort Worth basin: Clay, Montague, Jack, Wise, Denton, Palo Pinto, Parker, Tarrant (Figs. 2 and 4). I obtained raster images of gamma ray logs from 131 vertical wells in the study area from IHS, Inc. The images were loaded into a software package (Petra®) with functionalities for picking formation tops, making isopach and structure maps, and plotting cross sections. I selected the gamma ray log from the Mitchell Energy William Tedrow #4 in Wise County as the type log for my study (Fig. 5). I identified six prominent gamma ray spikes on the type log and correlated them throughout the eight-county area. I then made structure contour maps on the base of the Barnett Shale and each of the gamma ray spikes (GRS). I also made structure contour maps for the top of the Forestburg shale and the Forestburg limestone. An isopach was made for the interval between the base of the Barnett and the lowermost gamma ray spike (GRS-1) and for each of the intervals defined by the gamma ray spikes, for example GRS-1 to GRS-2, etc. Isopach maps were also made for the Forestburg limestone and the Forestburg shale.

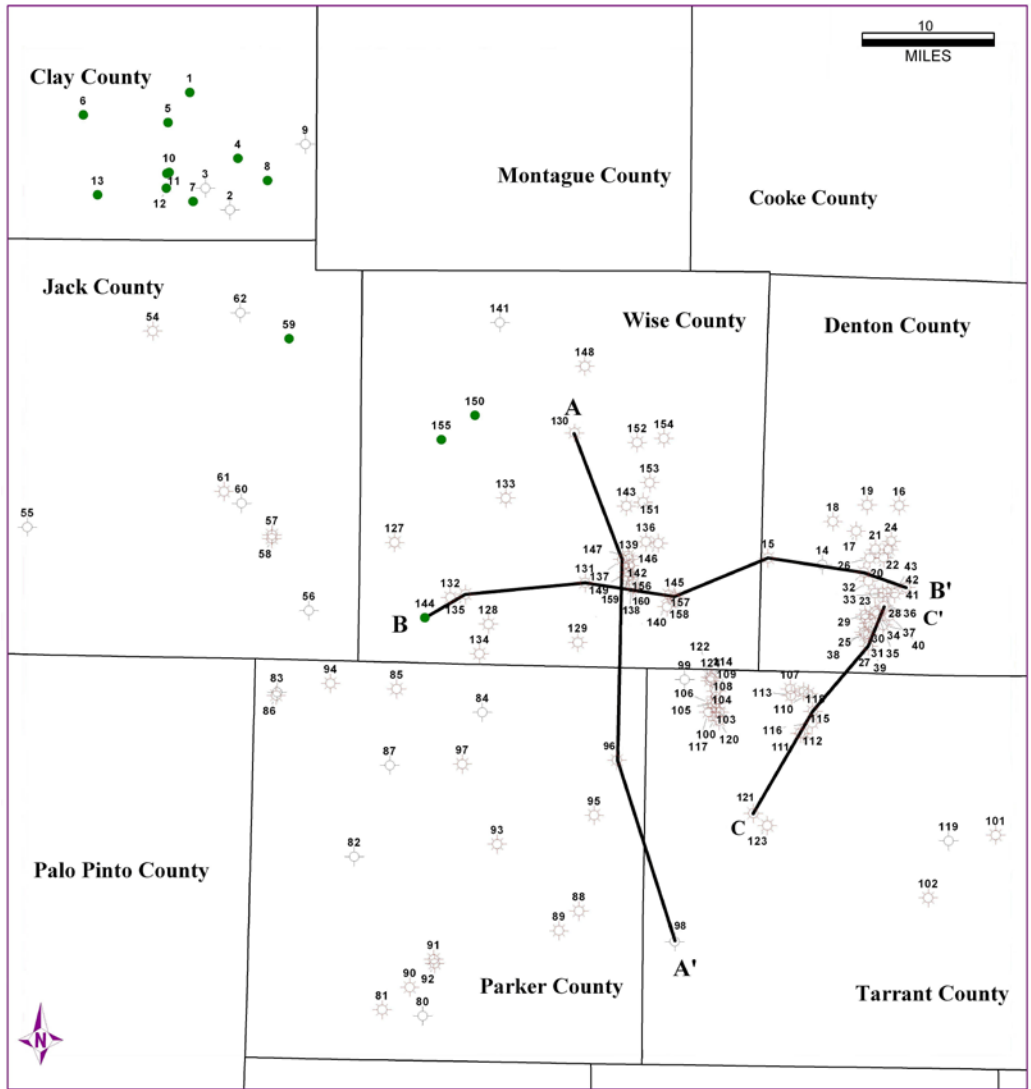


**Figure 4.** Map of the study area showing well control and location of cross sections. See Appendix I for names of the oil and gas wells.

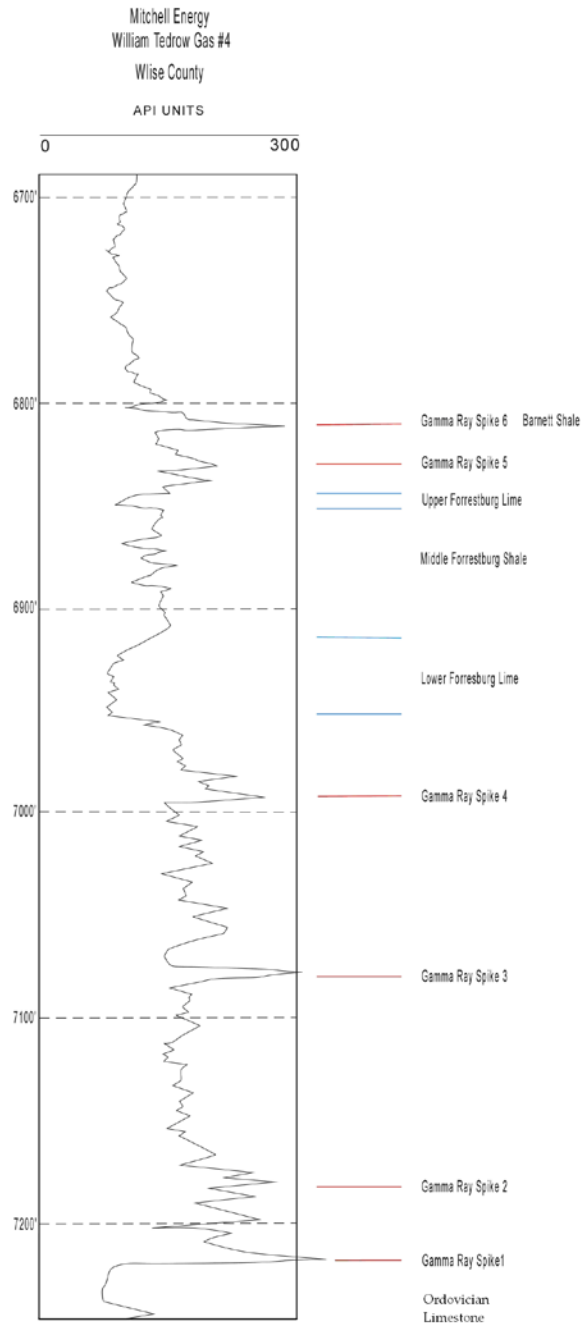


**Figure 5.** Type log for the study area showing the gamma ray spikes used to subdivide the Barnett Shale.

## **RESULTS**

### **Gamma Ray Spikes**

The Barnett Shale (Mississippian) is easily differentiated from the overlying Pennsylvanian strata (Morrowan and Atokan) and the underlying Ordovician strata (Viola Limestone or Ellenburger Group carbonates) by its high gamma ray count. The top of the Barnett is picked at an especially strong gamma ray excursion following some several thousand feet of mainly clastic strata. Spectral gamma ray logs from a well in the central part of the basin, whose location is proprietary, show the typical pattern. Shales in the overlying Pennsylvanian strata have total gamma ray counts ranging from 110 to 120 API units and uranium-free gamma ray counts of about 90 API units.

The gamma ray spike used to mark the top of the Barnett has a total gamma ray count exceeding 300 API units and a uranium-free gamma ray count exceeding 150 API units. The gamma ray counts within the Barnett are variable. In the well used as an example here, where the Barnett is 350 feet thick, over half the section has total gamma ray counts exceeding 180 API units. Gamma ray readings may drop as low as 75 API units in sharp spikes a few feet thick, perhaps in thin carbonate beds known within the Barnett at this location. Typically the lower third of the section has higher gamma ray readings than the upper part. The contact with the underlying Ordovician carbonates is also easily picked on gamma ray logs (Fig. 5). In this well the total gamma ray count fell from a sharp spike reading 165 API units to a thick section with readings of 15 to 30 API units (Fig. 5).

Gamma ray spike 1 (GRS-1) marks the contact with the underlying Ordovician carbonates (Fig. 5). GRS-6 marks the contact with the overlying Pennsylvanian strata, commonly the Marble Falls Limestone (Morrowan). These spikes, although varying in



their absolute intensity, typically are very strong and easily correlated throughout the study area. The gamma ray spikes in between GRS-1 and GRS-6 are commonly, but not always, of lesser intensity. The absolute intensity and the relative intensity of these spikes within the Barnett change throughout the study area. However, they can be correlated based on position in sequence and by using other distinctive log markers. In a given well, other gamma ray spikes may be more prominent than one or more of the six I chose to correlate, but attempts to correlate them throughout the study area were not successful.

### **Structure Contour Maps**

Previous work shows that in the study area the Barnett Shale rests on either the Viola Limestone or carbonates of the Ellenburger Group. The base of the Barnett was picked as the last gamma ray spike above a thick section of low gamma ray carbonates. The eroded edge of the Viola runs northwest to southeast along a line from eastern Johnson County, through western Tarrant County and central Wise County (Montgomery et al., 2005). West of this line the Barnett rests directly on the Ellenburger. The contact between the Barnett and underlying Ordovician strata is a slight angular unconformity ( $<1^\circ$ ) (Henry, 1982).

A structure contour map on the base of the Barnett Shale shows the topography of the eroded and karsted land surface flooded by the return of the sea to the Fort Worth basin in the Mississippian and its subsequent deformation (Fig. 6). The only major structural feature within the study area is the Mineral Wells fault, which extends some 65 miles across Palo Pinto, Wise and Denton counties. The fault trends northeast to southwest approximately parallel to regional dip. The trace of the fault could not be clearly delineated with the well control used in this study. Its precise location is taken

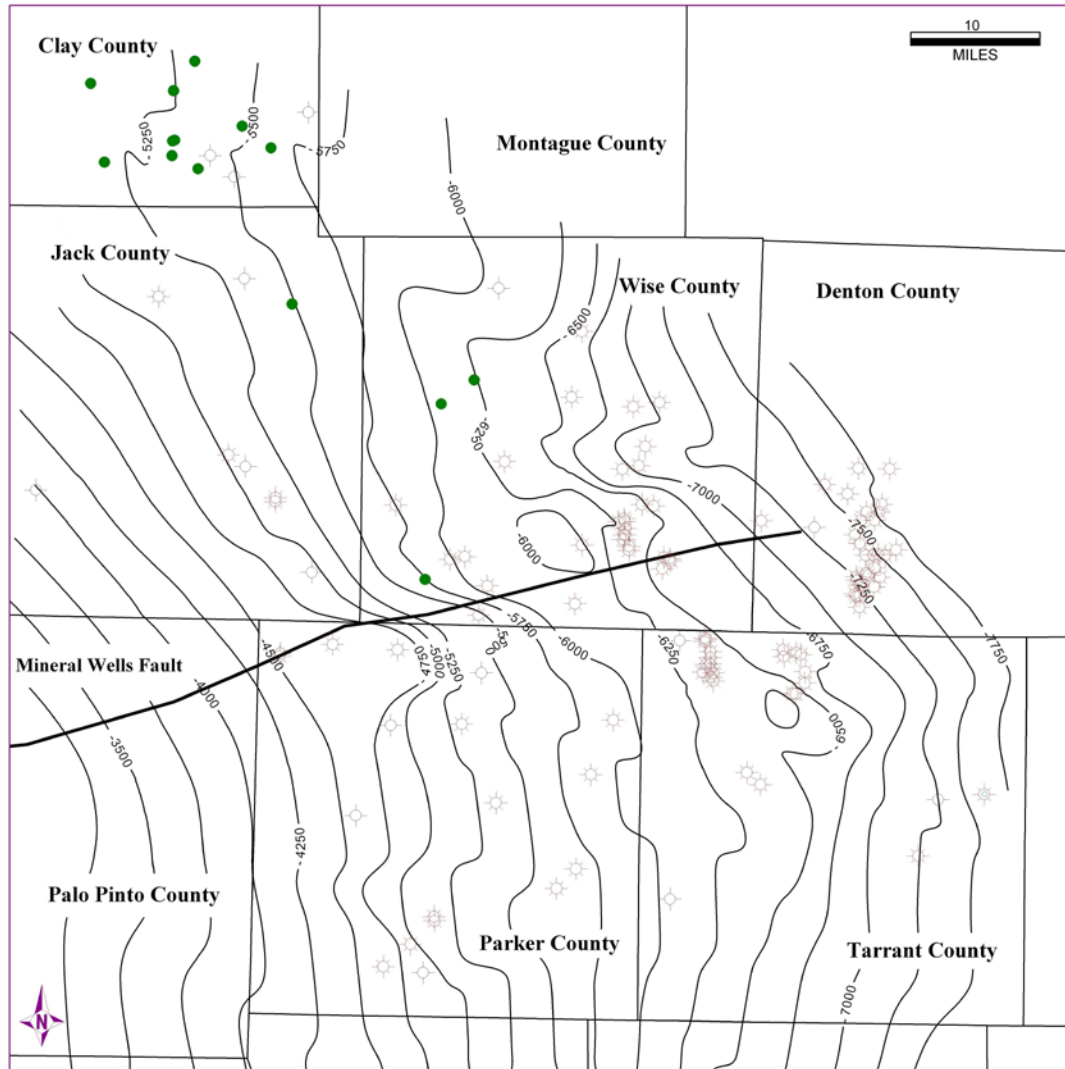


**Figure 6.** Structure contour map on the base of the Barnett Shale. Contour interval is 250 feet. The dark line is the Mineral Wells fault.

from the contour map on top of the Ellenburger given in Montgomery et al. (2005, their Fig. 1). [The fault is not apparent on the structure contour map on the top of the Ellenburger given by Pollastro et al. (2007, their Fig. 5) either.]

The base of the Barnett is found at elevations -5,250 feet to -3,250 feet along the western edge of the study area, from Jack County in the north to Palo Pinto County in the south. The elevation drops to -7,750 feet in central Denton County and -8,000 feet in Johnson County. Pollastro et al. (2007) show the base of the Barnett at more than 9,000 feet below sea level in northwestern Dallas County just outside my study area. The strike of the contours trends northwest-southeast in the northern part of the basin in Denton, Wise, and Jack counties, paralleling the Muenster Arch.

Strike swings to a more north-south direction in the southern tier of counties, where it runs along the Ouachita fold-thrust belt. The base of the Barnett drops over 4,000 feet in some 75 miles from central Palo Pinto County to the middle part of Denton County, giving a regional dip to the northeast of approximately  $0.6^\circ$ . Noticeably steeper dips are encountered along a northeast to southwest trending line across the southern half Wise County. These dip are found along southern edge of a low on the structure map that parallels the Mineral Wells fault system. Other than this feature the structure contour map is nearly featureless. A subtle high extends roughly east-west across northern Parker and Tarrant counties, but dies out in Palo Pinto County (Fig. 6). A low, which may be an artifact of data distribution runs from southeastern Clay County to the southeast through Wise County, eventually joining the low that parallels the Mineral Wells fault.

The other structure contour maps (Figs. 7-12) are broadly similar to the structure contour map on the base of the Barnett. The contours parallel the bounding elements of

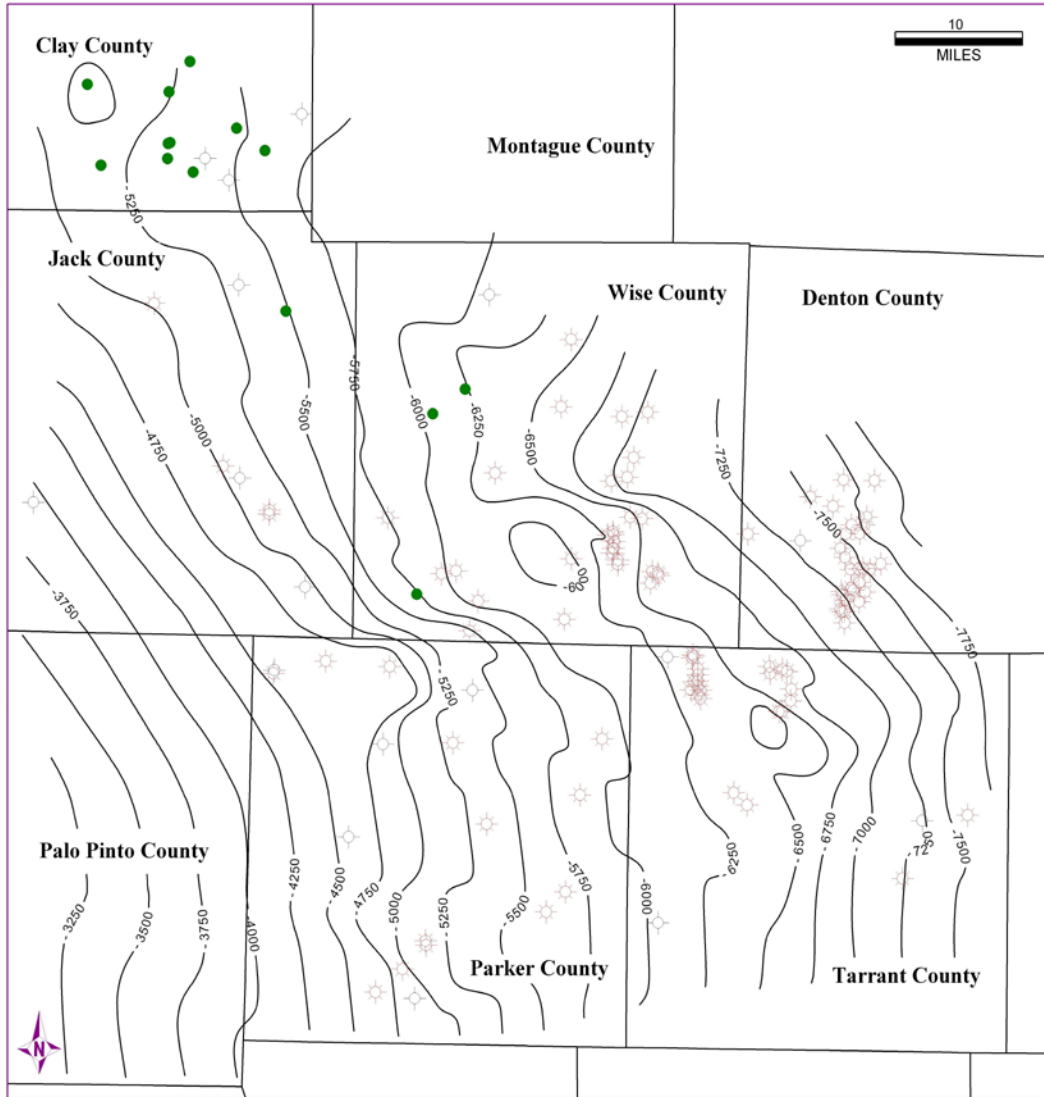


**Figure 7.** Structure contour map on GRS-1. Contour interval is 250 feet.

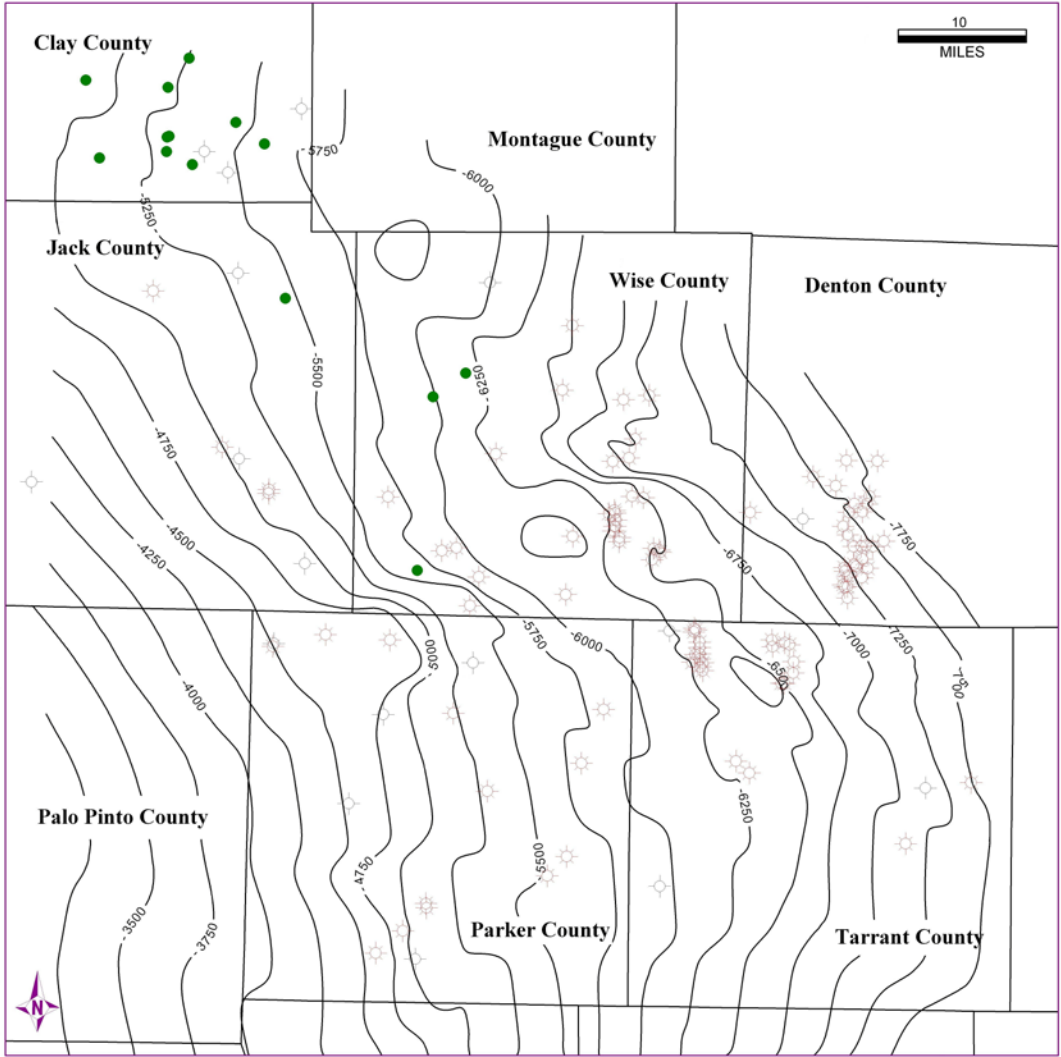


**Figure 8.** Structure contour map on GRS-2. Contour interval is 250 feet.

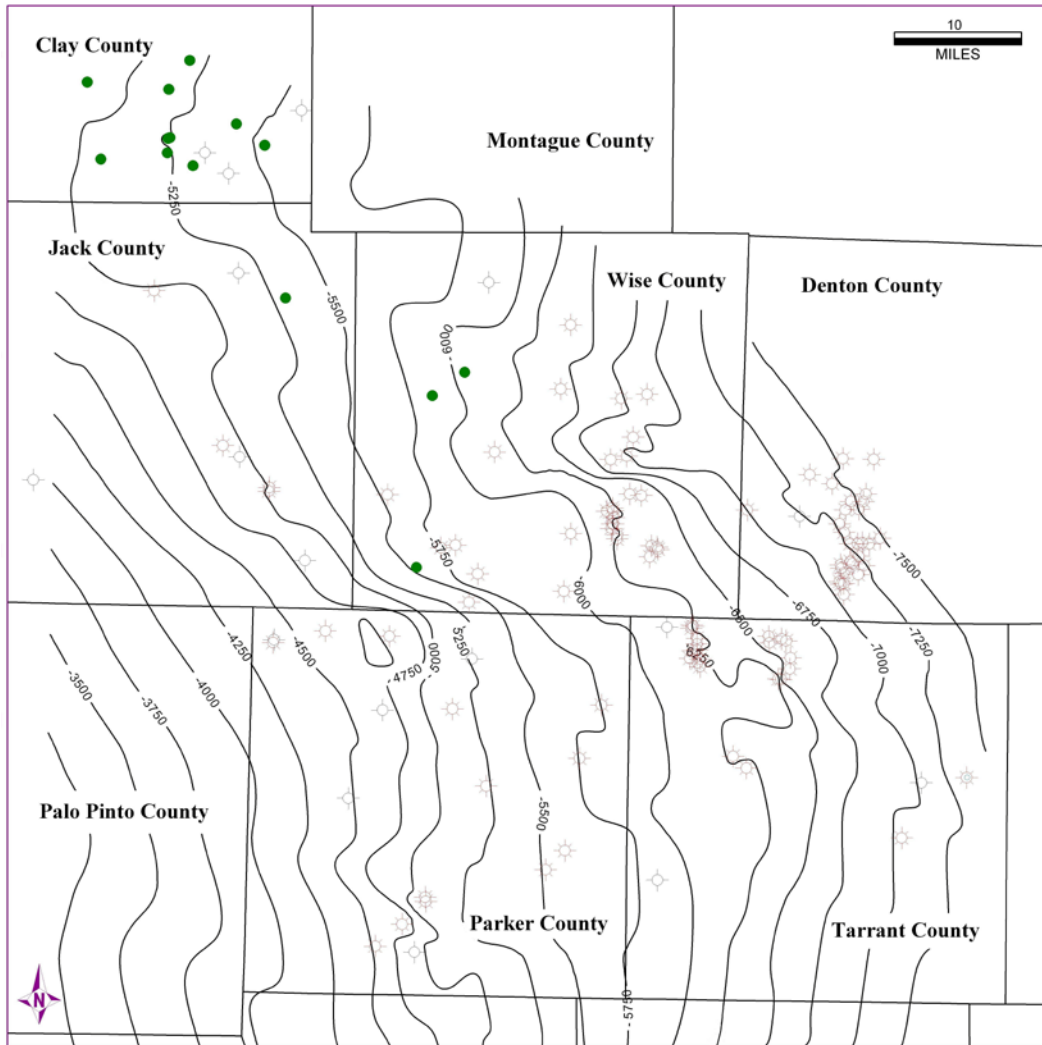


**Figure 9.** Structure contour map on GRS-3. Contour interval is 250 feet.

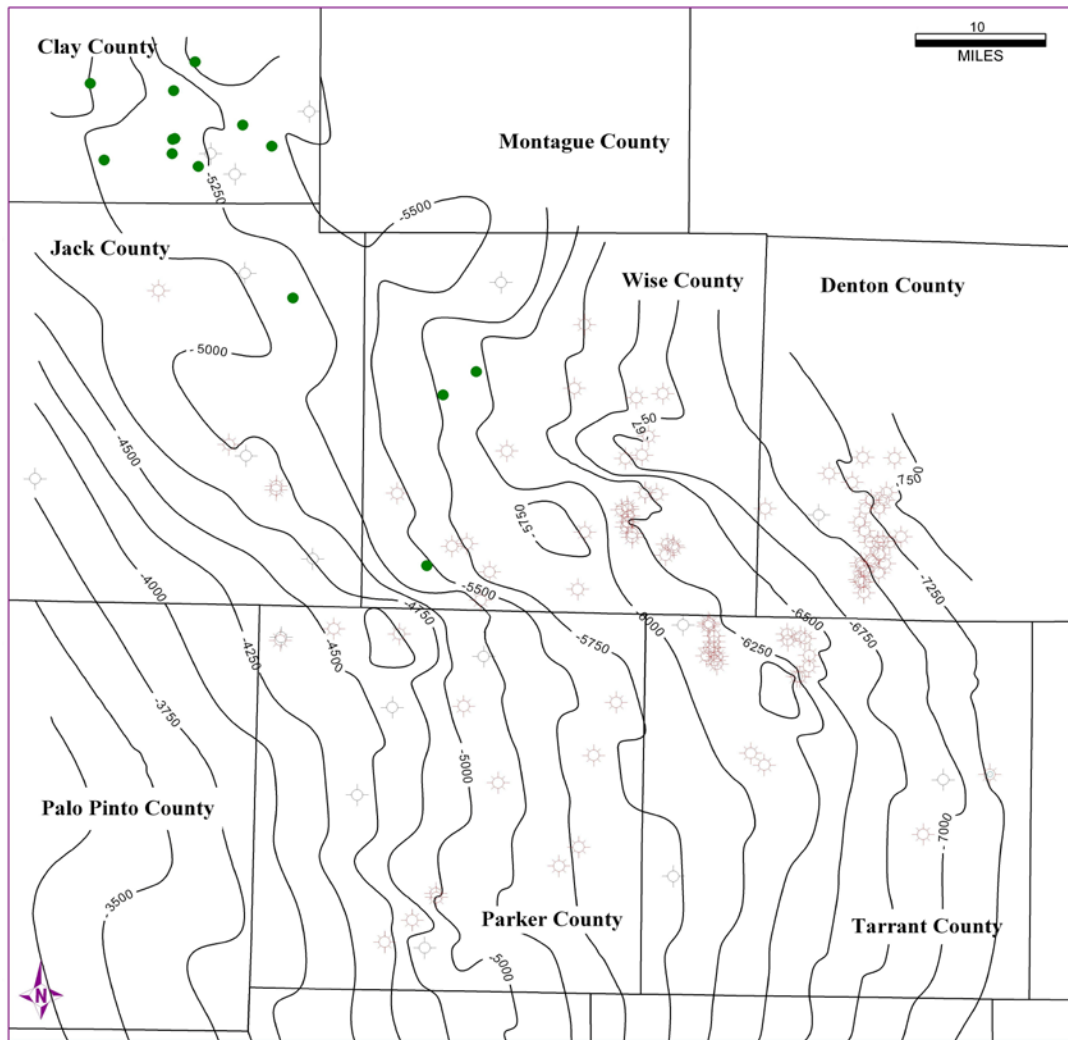


**Figure 10.** Structure contour map on GRS-4. Contour interval is 250 feet

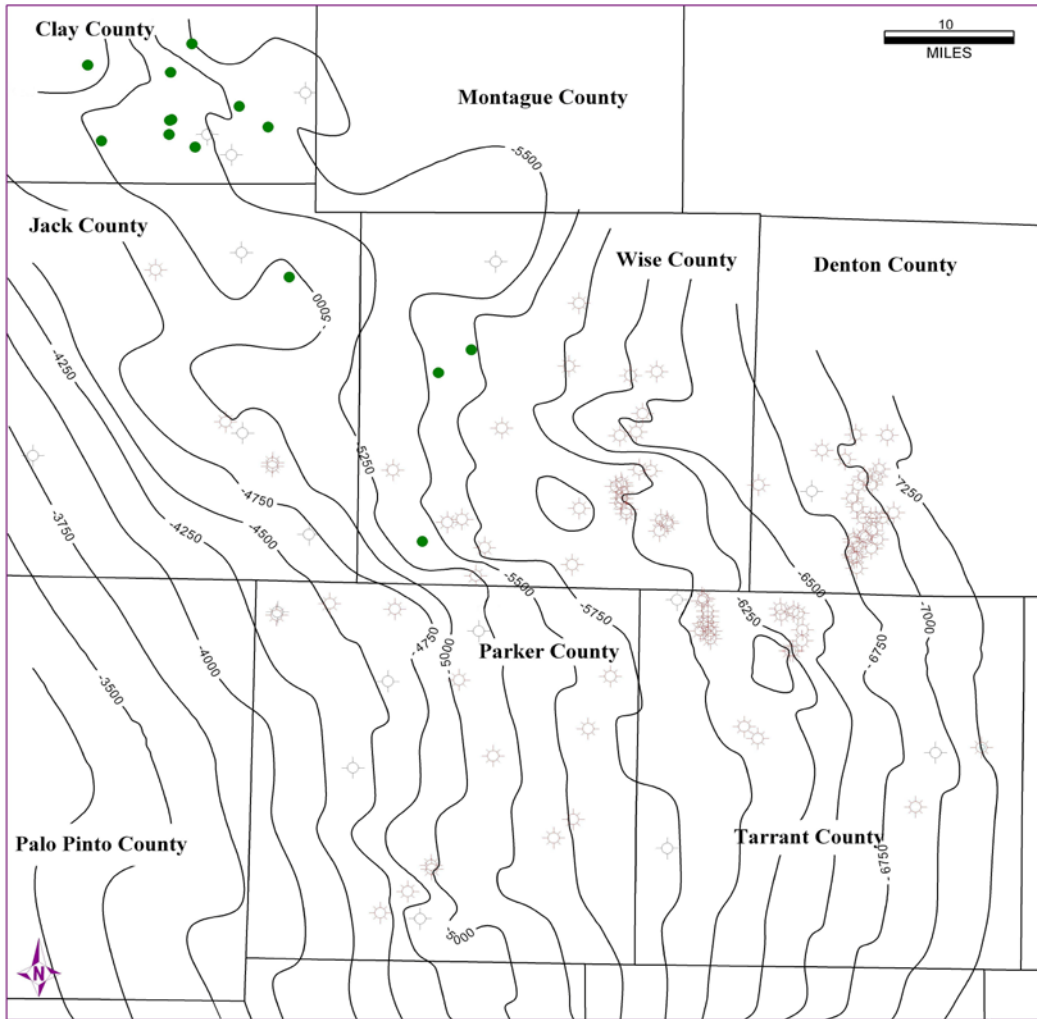


**Figure 11.** Structure contour map on GRS-5. Contour interval is 250 feet



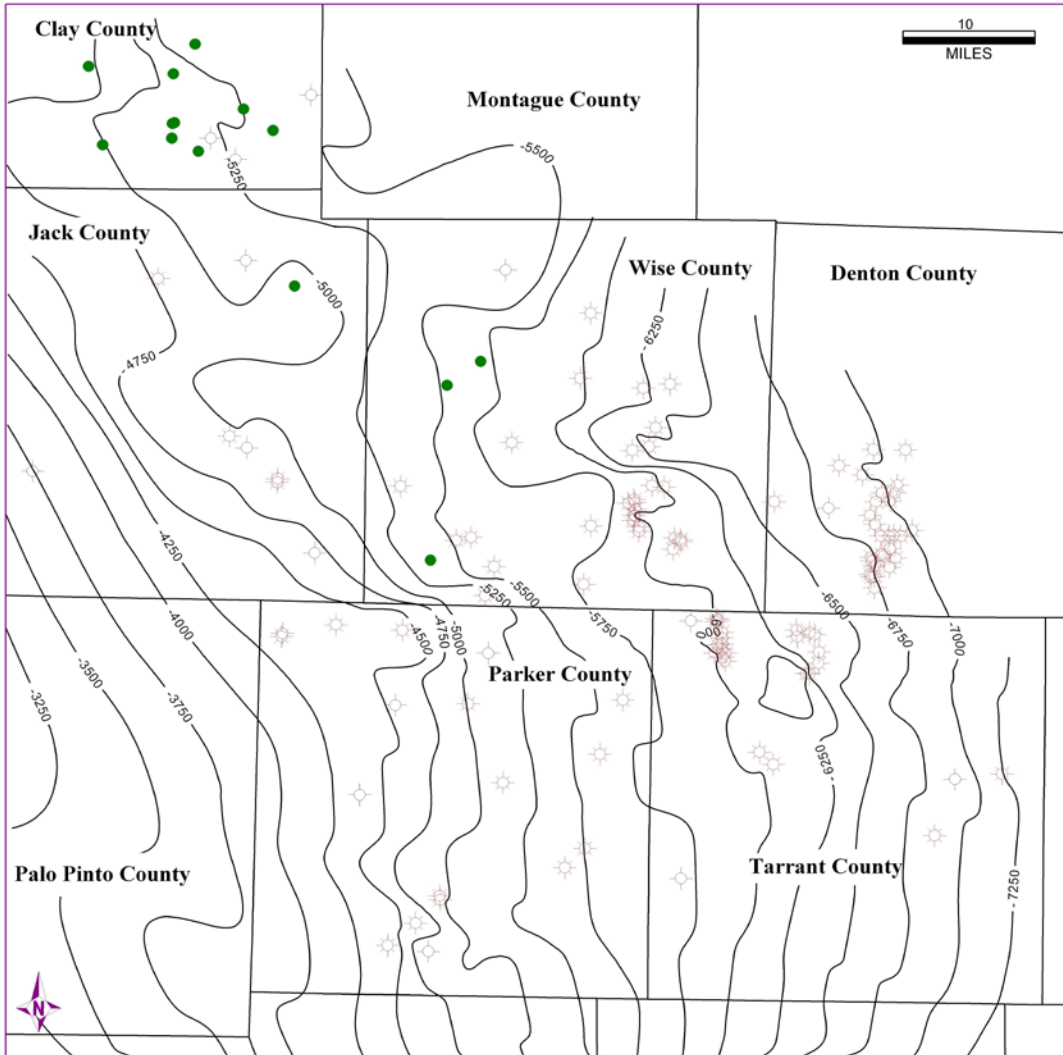


**Figure 12.** Structure contour map on GRS-6. Contour interval is 250 feet

the basin, trending northwest to southeast in Wise and Denton counties along the Muenster arch and then running north-south in Tarrant County along the Ouachita front. The northeast-southwest trending low in the southern half of Wise County is present on all the maps as is the broad, east-west trending high in northern Parker and Tarrant counties. A northwest-southeast trending low in southeastern Clay County and northwestern and central Wise County is present on all the structure maps as well. The regional dip is to the northeast in the northern tier of counties and to the east, and slightly southeast, in the southern tier of counties. The regional dip on the surfaces generally ranges from  $0.25^{\circ}$  to  $0.65^{\circ}$ .

Structure contour maps were also made on the top of the Forestburg limestone and the top of the Forestburg shale (Figs. 13 and 14). These units lie above GRS-4 and below GRS-5. The Forestburg shale separates the upper part of the Forestburg limestone from the lower part. Within the study area these units are found in the northern tier of counties (Jack, Wise, Denton) and the northern portions of Parker and Denton counties. Both units pinch out to the south and west. The structure maps resemble those for the other surfaces. The strike is northwest-southeast in western Denton County and eastern Wise County parallel to the Muenster arch. To the west, strike turns north-south to run parallel to the Bend Arch. Regional dip is to the east at less than  $1^{\circ}$ . A structural low runs east-west through central Wise County. The similarity of all the structure contour maps indicates that no differential tectonic movement took place in the Fort Worth basin during the deposition of the Barnett Shale.

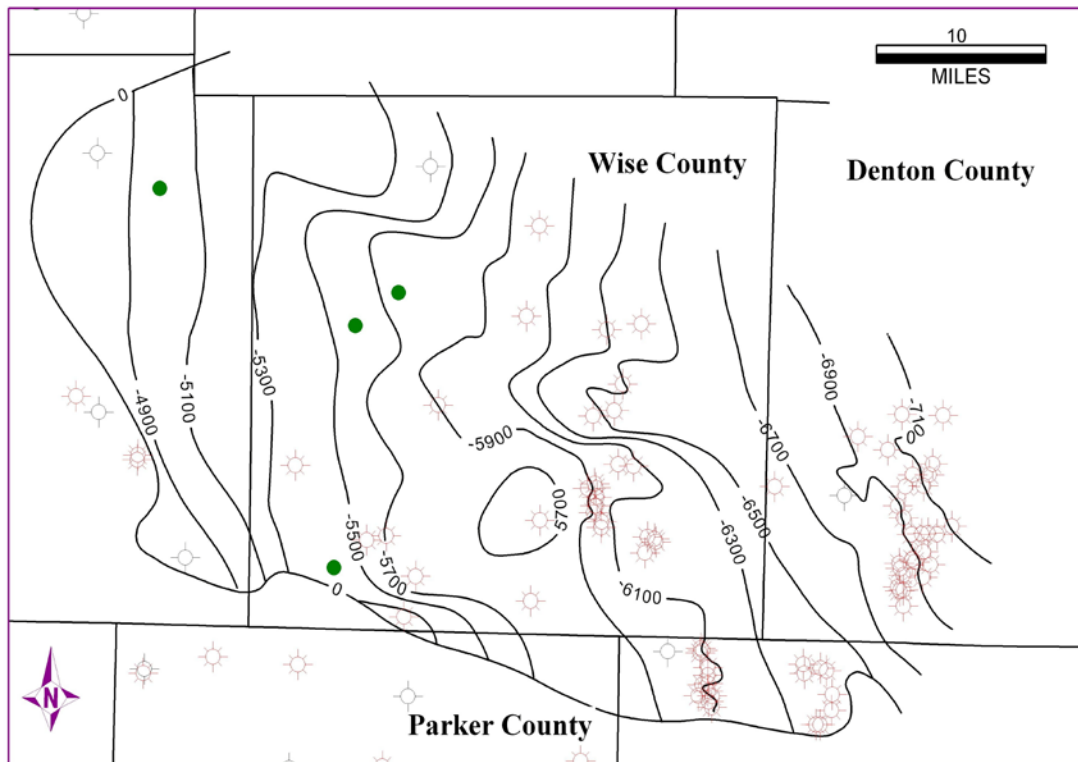


**Figure 13.** Structure contour map on top of the Forestburg limestone. Contour interval is 200 feet

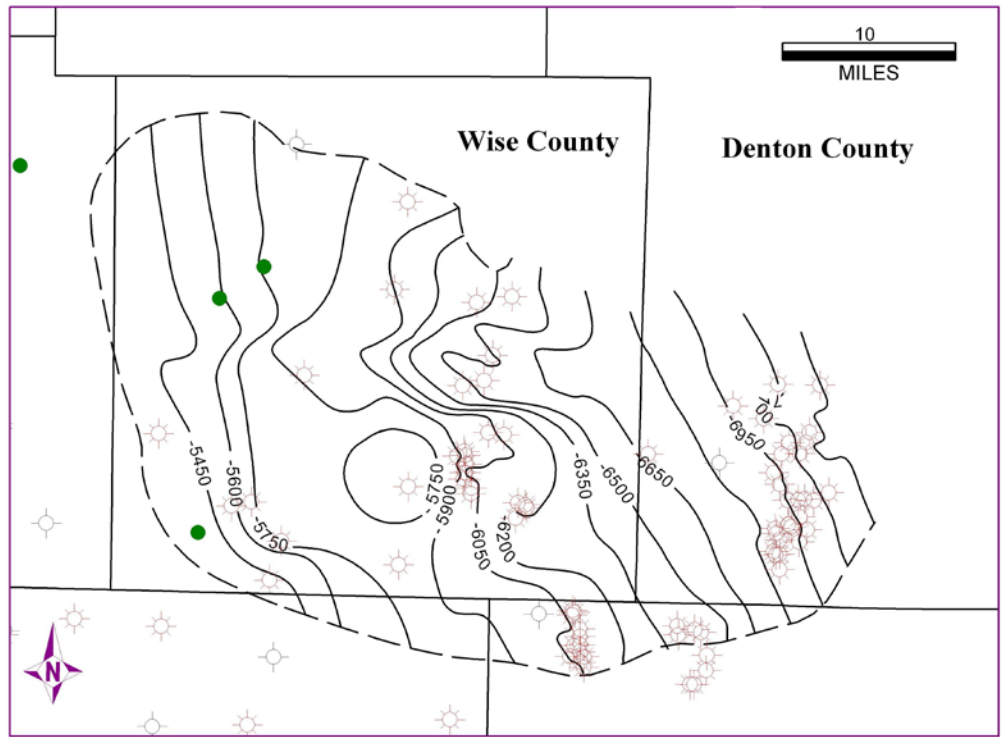


**Figure 14.** Structure contour map on top of the Forestburg shale. Contour interval is 150 feet.

## Isopach Maps

Over most the study area the thickness from the base of the Barnett Shale to the lowermost gamma ray spike (GRS-1) is less than 5 feet (Fig. 15). In the northeastern part of the study area the sediments responsible for GRS-1 lie directly on the underlying limestone and this interval thins to zero. Nowhere is the interval from the base of the Barnett to GRS-1 thicker than 25 feet. A linear feature, with isopach values ranging from 5 to 20 feet thick, extends northwest to southeast from southwestern Wise County across northern Tarrant County. The interval between GRS-1 and GRS-2 thickens from northwest to southeast across the study area (Fig 16). This interval ranges from 40 feet to 80 feet over most of the area, and reaches a maximum thickness of more than 120 feet in southeastern Tarrant County.

The interval between GRS-2 and GRS-3 is thicker than the lower intervals (Fig. 17). The contours show a pronounced trend from northwest to southeast, approximately parallel to the Muenster arch. The interval thickens to the northeast into the deepest part of the Fort Worth basin. The thickness increases from 25 feet in northeastern Palo Pinto County to more than 125 feet in southeastern Denton County. A pronounced isopach thick extends along the southern boundary of Tarrant County. Here the interval is up to 200 feet thick.

The thickness between GRS-3 and GRS-4 also increases from southwest to northeast into the deepest part of the basin (Fig. 18). As in the interval immediately below, the contour lines run northwest to southeast paralleling the Muenster arch. The thickness changes gradually from 75 feet to 150 over 20 miles from southeastern Wise County to central Wise County. The thickness then increases to 250 feet over a



**Figure 15.** Isopach map of the interval between the base of the Barnett Shale and GRS-1. Contour interval is 5 feet.



**Figure 16.** Isopach map of the interval between GRS-1 and GRS-2. Contour interval is 20 feet.

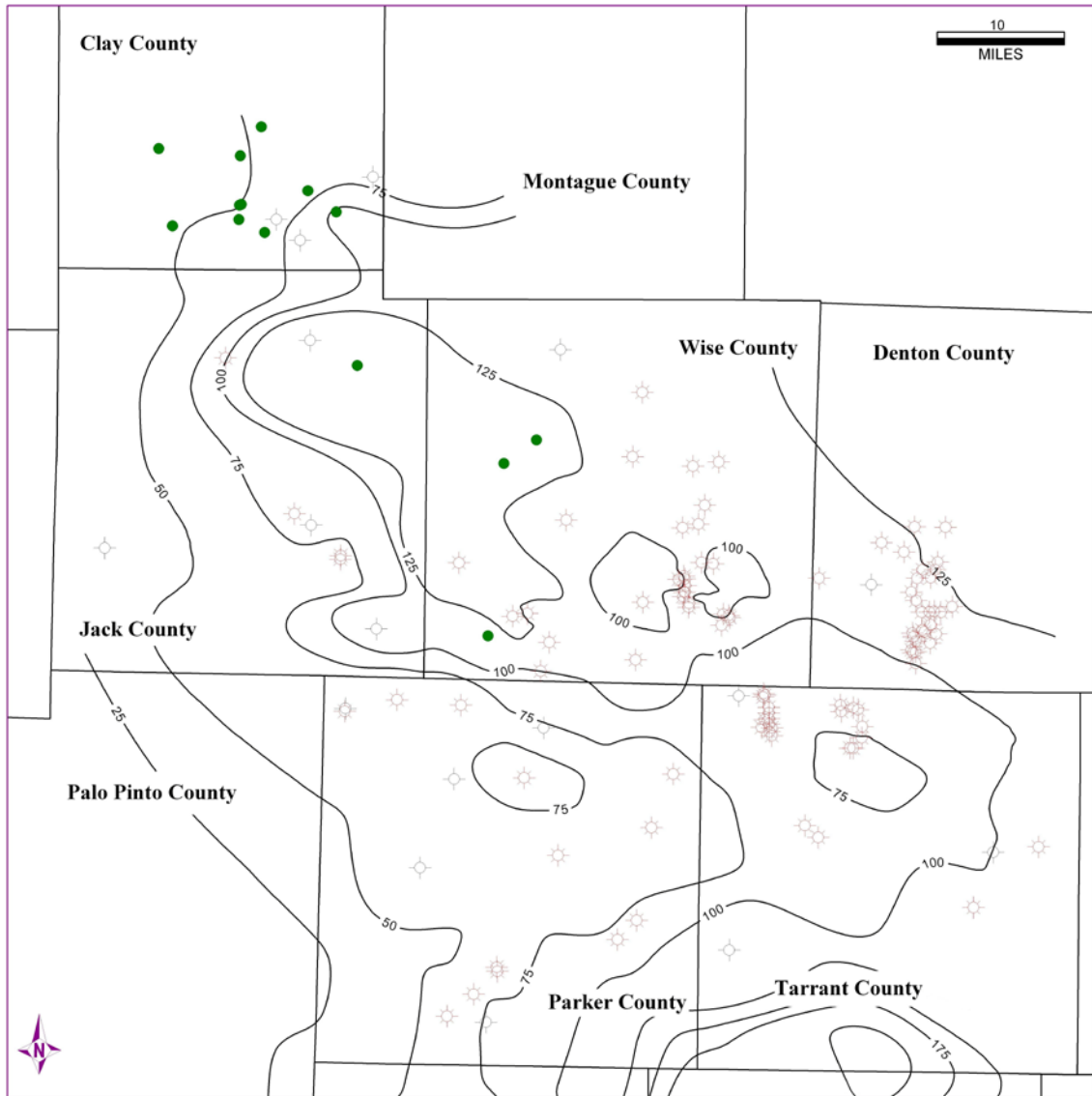


**Figure 17.** Isopach map of the interval between GRS-2 and GRS-3. Contour interval is 25 feet.



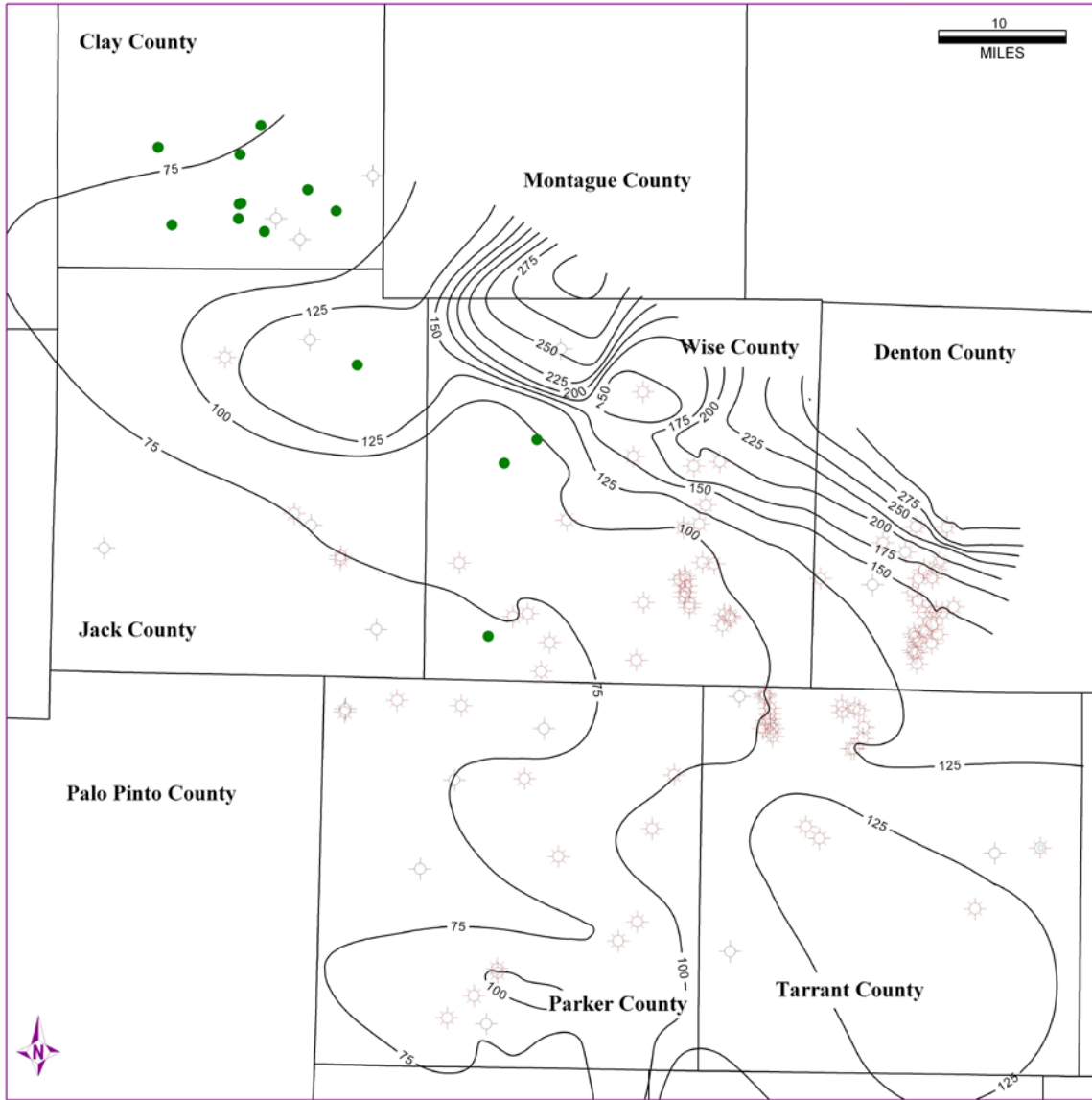


**Figure 18.** Isopach map of the interval between GRS-3 and GRS-4. Contour interval is 25 feet.

distance of less than 5 miles. This sharp change in the rate of increase is marked by the closely spaced contours running from the northwest corner of Wise County into the central part of Denton County.

The interval between GRS-4 to GRS-5 includes the Forestburg limestone. The interval thickens from southwest to northeast, reaching a maximum thickness of over 300 feet in northeastern Wise County (Fig. 19). Over most of the southern tier of counties (Palo Pinto, Parker, Tarrant), where the Forestburg pinches out, this interval is less than 25 feet thick. It shows a rapid increase in thickness along a northwest-to-southeast trending hinge that runs from northeastern Jack County through Wise County to southwestern Denton County.

The interval from GRS-5 to GRS-6 is much thinner than the interval from GRS-3 to GRS-4 (Fig. 20). It reaches a maximum thickness of less than 50 feet in northern Parker County. The orientation of the isopach contours is also quite different. The contours trend approximately east-west, rather than northwest-southeast (the trend also seen in the Forestburg limestone). An isopach thick extends across the northern part of Parker County and into Tarrant County.

In this study, the Forestburg limestone is divided into three parts: an upper limestone and a lower limestone separated by a shale (Fig. 5). The Forestbug limestone is restricted to the northern part of the Fort Worth basin. In the study area it is thickest in central Wise County where it is more than 200 feet thick (Fig. 21). From here, the Forestburg interval thins rapidly to the south and west. It pinches out in eastern Jack County and northern Parker and Tarrant counties. As in most of the other intervals in the

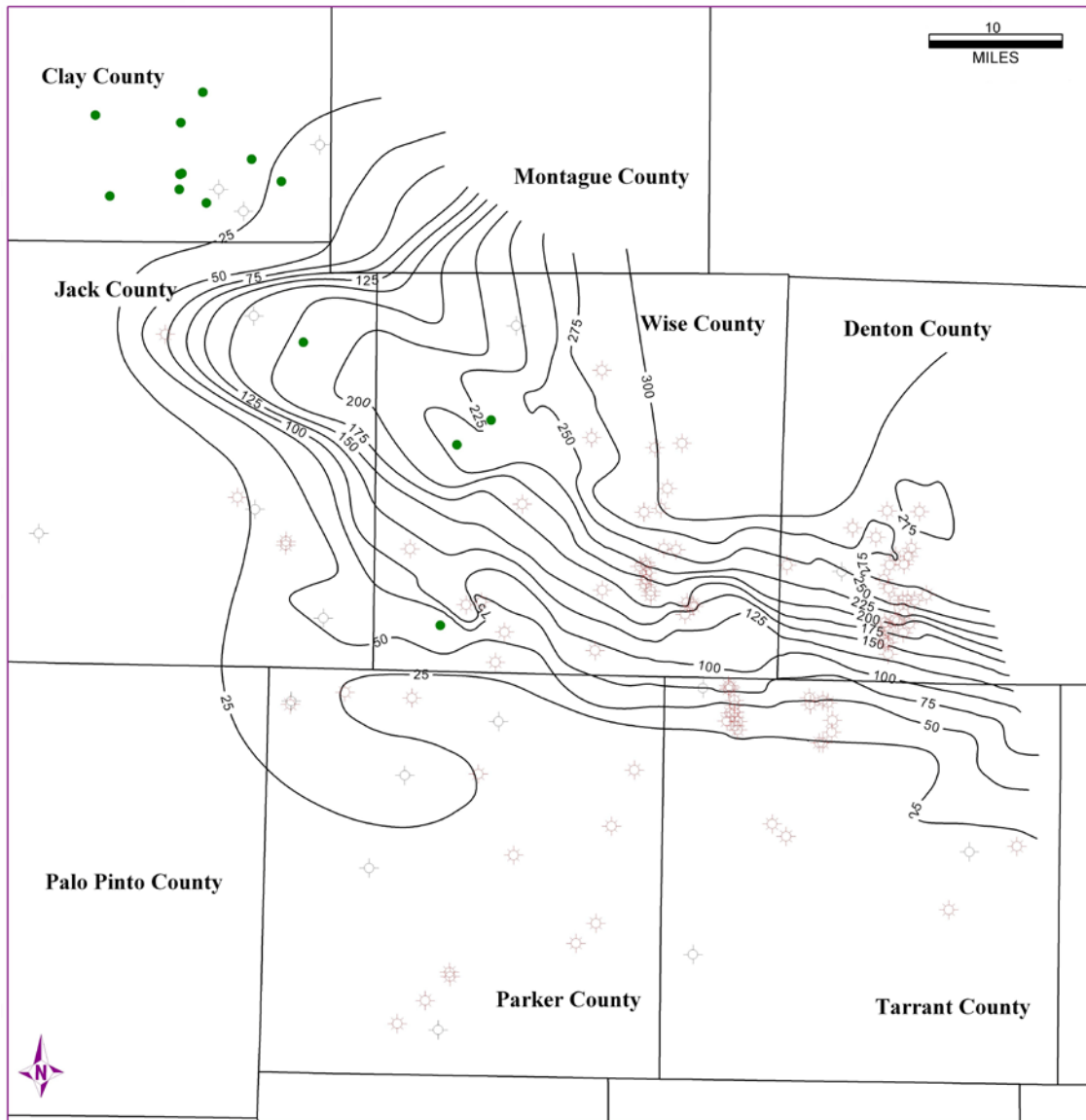


**Figure 19.** Isopach map of the interval between GRS-4 and GRS-5. Contour interval is 25 feet.

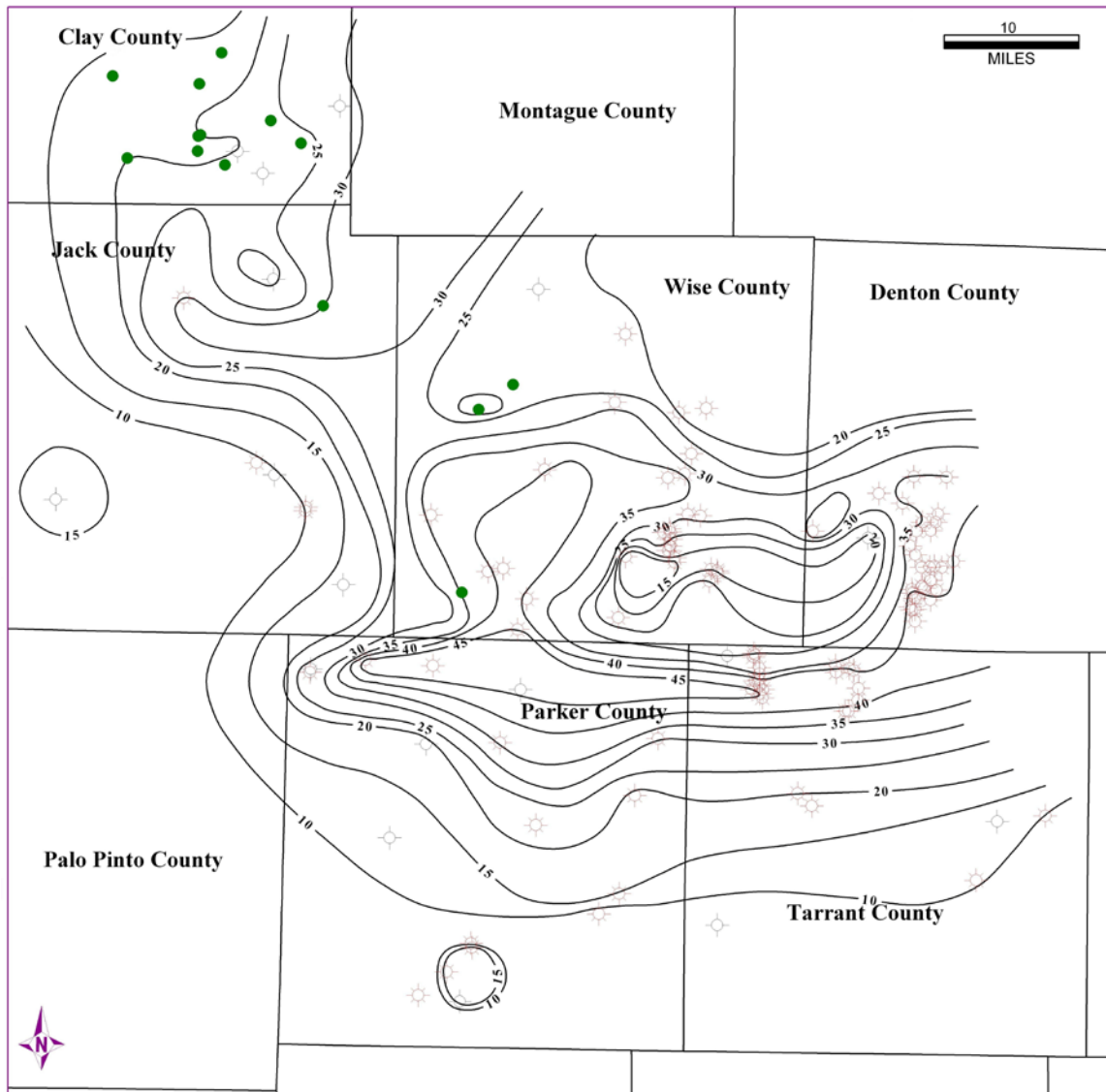


**Figure 20.** Isopach map of the interval between GRS-5 and GRS-6. Contour interval is 5 feet.

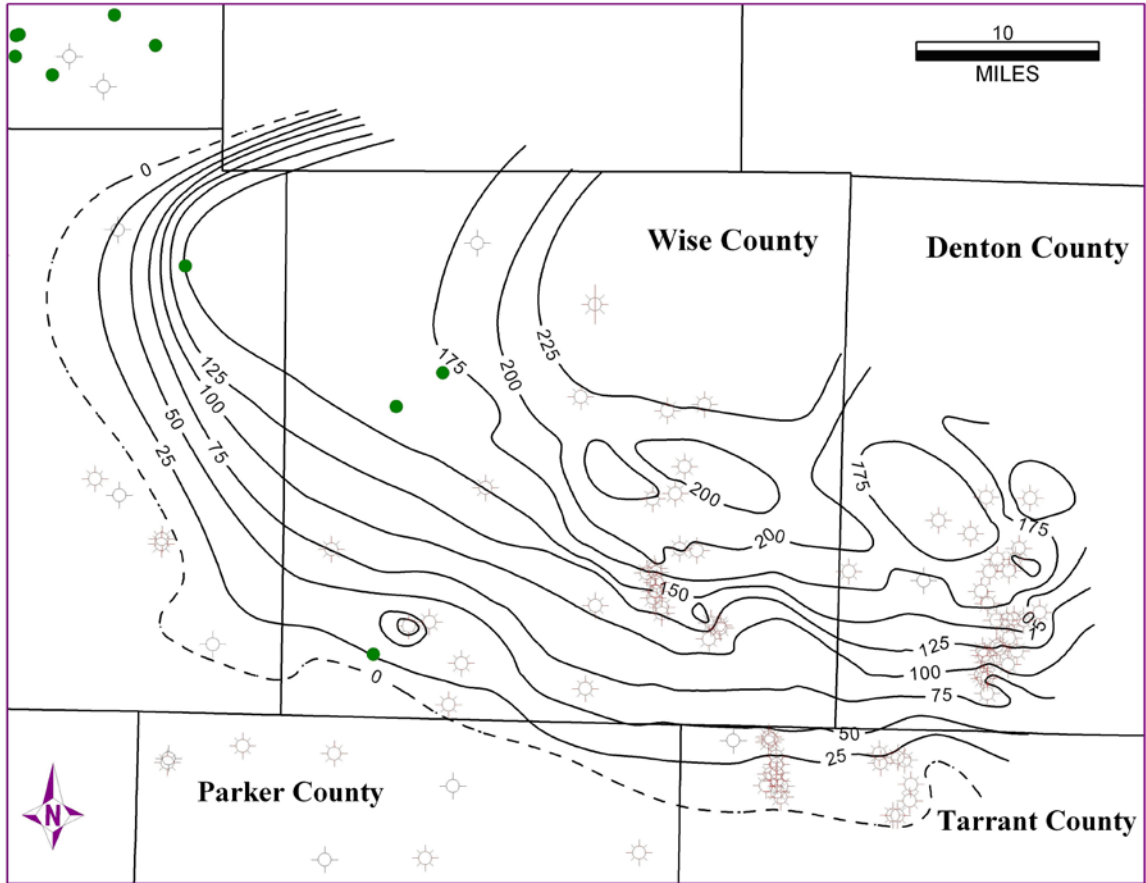


**Figure 21.** Isopach map of the entire Forestburg limestone, including the upper, middle and lower units. Contour interval is 25 feet.

Barnett, the contours on the isopach map trend northwest to southeast paralleling the Muenster arch.

### **Cross Sections**

Three well log cross-sections were made across the study area (Fig. 4 and plates in pocket). Cross-section A-A' runs from north to south approximately parallel to the strike of the Barnett Shale. The cross section shows logs from Rowan Drilling's B. L. Markum #1, Range Production Company's Seven Knolls #1, and Mitchell Energy's T. W. Perkins #4 and Bum Johnson #2. The six gamma ray spikes and the Forestburg limestone are correlated across the section.

After the first gamma ray spike directly above the Ordovician unconformity there is a relatively thin lowstand deposit. Above the lowstand deposits in the southern wells of this cross section is a gradual increase in the gamma-ray intensity. This retrogradational stacking pattern leads to the second maximum flooding surface. In the northwestern portion of the basin the second transgressive systems tract thins considerably, and the retrogradational stacking pattern is not present.

Between the five other condensed sections in the Barnett shale there are mainly lowstand deposits. Lowstand deposits in the cross sections are defined by lower gamma-ray readings, and by blocky log patterns with sharp bases. Between the main gamma-ray spikes there are parasequences of lower gamma ray values that show blocky log signatures. Within sequences three and four are significant gamma ray spikes that represent fourth-order flooding surfaces between the lowstand parasequences.

Apart of the fourth lowstand deposit there is the Forestburg limestone, which is a classic debrite. Parasequences in this sequence aggraded until the fifth maximum flooding surface. To the south the Forestburg limestone disappears. Beyond this point the lowstand deposits in the fourth sequence along with the entire Barnett thin considerably (Plate 1).

Cross-section B-B' runs west to east approximately parallel to regional dip. This cross section includes Republic Energy's Lee Luther #2, Mereken Energy's Obenchain #1, and Mitchell Energy's M. E. Pruett #1, J. S. Adams #3, Young Margaret #3, William Dedrow #4, and Graham Ranch #1. In this cross section the transgressive systems tract below the second maximum flooding surface can be seen in all the wells. This cross section also shows prolonged lowstand deposits in the third and fourth sequences. The lowstand Forestburg limestone in this cross section is split into upper and lower units that are separated by a minor shale member. The source of the Forestburg sediments was the Muenster arch to the northeast (Plate 2).

Cross-section C-C' also shows rapid changes in the thickness of Forestburg limestone along the eastern part of the study area. This cross section includes Antero Resources' Hayco #2H, Dan Meeker Management's Bagby #1, Four Seven's Golden Triangle #1, Devon Energy's Byron Nelson #1, and Republic Energy's Gail Ewing #3. It also shows the distinct transgressive stacking pattern above the first thin lowstand deposits. Again above the pronounced third maximum flooding surface is a series of aggrading lowstand packages that are separated by smaller order flooding surfaces (Plate 3).

## Discussion

Deposition of the Barnett Shale took place during a prolonged second-order highstand of eustatic sea level during the Late Mississippian (Ross and Ross, 1988, their Fig. 9). In the northern Fort Worth basin, the Barnett Shale accumulated beneath 400 to 700 feet of water (Loucks and Ruppel, 2007). The bottom waters were anaerobic to dysaerobic, allowing organic matter to accumulate.

Terrigenous sediment was transported to basinal settings by hemipelagic plumes and turbidity currents. Sedimentation rates within the basin fluctuated with third-order cycles of change in relative sea level. Gamma ray spikes in the Barnett represent condensed sections formed during maximum flooding of the shelf. These spikes represent periods of extremely slow sedimentation (Loutit et al., 1988). Deposits formed at these times would be rich in chemogenic and biogenic sediment, and also high in TOC, because the organic matter accumulating on the sea floor was not diluted by terrigenous debris. During lowstands the Fort Worth basin received greater amounts of terrigenous debris and normal basinal sediments accumulated.

Uranium associated with organic matter and phosphatic debris produces higher gamma ray counts in condensed sections than in the more argillaceous shales deposited above and below them. Spectral gamma ray logs suggest that high gamma ray counts in the Barnett Shale are associated with increased concentrations of uranium. For this reason, I interpret six gamma ray spikes in the Barnett Shale in the northern Fort Worth basin as condensed sections formed during maximum flooding of the shelf during third-order changes in relative sea level.



These maximum flooding surfaces separate sediments of the transgressive systems tract below the condensed section from those of the highstand systems tract above the condensed section. In nearshore and inner shelf settings the highstand systems tract is overlain by the sequence-bounding unconformity formed on the falling limb of the relative sea level curve. The unconformity dies out basinward and is replaced by its correlative conformity. I could not detect a distinct log signature for the correlative conformity in the basinal shales. Similarly, I could not find a log signature that could be identified with the transgressive surface that separates the lowstand systems tract from the highstand systems tract. In basinal settings both the correlative conformity and the transgressive surface will lie in continuous sequences of pelagic and hemipelagic sediment. No lithologic basis for a distinctive log signature exists

Parasequence stacking patterns provide another means of identifying systems tracts on the relative sea level curve (Van Wagoner et al., 1990, among others). The transgressive systems tract is often characterized by a retrogradational stacking pattern. The early highstand systems tract frequently shows an aggradational stacking pattern and the late highstand, progradational. Parasequences above each maximum flooding event in the Barnett show mostly aggradational stacking patterns. Typically, following the most pronounced gamma ray spike the logs used in my study show a decrease in gamma ray intensity, which represents increased sedimentation into the basin and dilution of the uranium-rich organic matter. Aggradation after the maximum flooding surface is a succession of lower gamma ray values that were separated by lesser gamma ray peaks of approximately equal magnitude.

The gamma ray intensity on the logs sometimes increased gradually leading up to each maximum flooding surface. Gradual gamma ray increases before the maximum flooding surface represent parasequences with retrogradational stacking patterns. There are significant drops in the gamma ray intensity, which I attribute to dilution of uranium-bearing organic matter by argillaceous debris derived from the Chappel shelf or Muenster arch. After the sea level fall following the first maximum flooding event the gamma ray log shows a steady and gradual increase in intensity. This continues until the apex is reached at the second maximum flooding event.

Above the third maximum flooding event in the Barnett is a series of very high gamma ray spikes, indicating a marked decrease in the input of terrigenous sediment. Sea level was high, trapping sediment along the shoreline. Accommodation space in the Fort Worth basin would have been higher during this phase of the Mississippian than at any other time. Sea level then increased again to create the fourth maximum flooding condensed section.

The maximum flooding surfaces in the upper part of the Barnett are more closely spaced than the surfaces in the lower part of the Barnett. Either the third-order cycles of relative change in sea level were shorter, or the sedimentation rate was lower at this time than earlier in the history of the basin.

### **Conclusions**

The Barnett Shale was deposited in a deep, anoxic basin during the Mississippian. Significant amounts of organic matter accumulated along with siliceous microscopic organisms and argillaceous material derived from nearby landmasses.

Fine-grained was deposited in a sea separating the approaching continents of Gondwana and Laurussia.

Deposition of this fine-grained lasted for nearly twenty-five million years. Sediments were deposited in this sea through pelagic and hemipelagic processes, along with debris flows and turbidity currents from surrounding shelf areas. During the deposition of the Barnett shale sea level fluctuated many times; and, during periods of sediment starvation, condensed sections were produced. Condensed sections are presumably a product of maximum flooding events, and can be correlated across the Fort Worth basin using primarily the gamma ray log.

I analyzed well over a hundred gamma ray logs from wells in the northern part of the Fort Worth basin. I identified six maximum flooding surfaces during the deposition of the Barnett (Plates 1 through 3 and Fig. 5). Between each of these maximum flooding surfaces are parasequences displaying the typical stacking patterns recognized in studies of sequence stratigraphy. Retrogradational stacking patterns are seen below the maximum flooding surfaces. Aggradational and/or progradational stacking patterns are seen above the maximum flooding surfaces. Lowstands were recognized on the gamma ray logs by especially low API counts.

## REFERENCES

- Baturin, G. N., 1982, Phosphorites on the sea floor: Origin, composition, and distribution: New York, Elsevier Scientific, 343 p.
- Beers, R. B., 1945, Radioactivity and organic content of some Paleozoic shales: American Association of Petroleum Geologists Bulletin, v. 29, p. 1-22.
- Blakey, R., 2005, Paleogeography and Geologic Evolution of North America—images that track the ancient landscapes of North America:  
<http://jan.ucc.nau.edu/~rcb7/nam.html> (accessed December 20, 2008).
- Bohacs, K. M., 1998, Contrasting expressions of depositional sequences in mudrocks from marine to non marine environs, *in* Schieber, J., W. Zimmerle, and P. S. Sethi, Shales and Mudstones I—Basin Studies, Sedimentology, and Paleontology: Stuttgart, E. Schweizerbart'sche Verlagsbuchhandlung, p. 33-78.
- Bunting, P. J., Petrographic analysis of the Barnett Shale in the Fort Worth basin: Master's thesis, Texas Christian University, Fort Worth, Texas, 101 p.
- Cheney, M. G., 1940, Geology of north-central Texas: American Association of Petroleum Geologists Bulletin, v. 24, p. 65-118.
- Creaney, S., and Q. R. Passey, 1993, Recurring patterns of total organic carbon and source rock quality within a sequence stratigraphic framework: American Association of Petroleum Geologists Bulletin, v. 77, p. 386-401.
- Flawn, P. T., A. Goldstein, Jr., P. B. King, and C. E. Weaver, 1961, The Ouachita System: University of Texas at Austin, Bureau of Economic Geology, Publication 6120, 401 p.

- Flippin, J. W., 1982, The stratigraphy, structure, and economic aspects of the Paleozoic strata in Erath County, north central Texas, *in* Martin, C. A., ed., Petroleum Geology of the Fort Worth Basin and Bend Arch Area: Dallas Geological Society, p. 129-155.
- Henry, J. D., 1982, Stratigraphy of the Barnett Shale (Mississippian) and associated reefs in the northern Fort Worth basin, *in* Martin, C. A., ed., Petroleum Geology of the Fort Worth Basin and Bend Arch Area: Dallas Geological Society, p. 157-178.
- Hickey, J. J., and Henk, B., 2007, Lithofacies summary of the Mississippian Barnett Shale, Mitchell 2 T. P. Sims well, Wise County, Texas: American Association of Petroleum Geologists Bulletin, v. 91, p. 437-443.
- Kier, R. S., L. F. Brown, E. F. McBride, 1980, The Mississippian and Pennsylvanian (Carboniferous) Systems in the United States—Texas: Bureau of Economic Geology, University of Texas at Austin, Geological Circular 80-14, 45 p.
- Loucks, R. G. and S. C. Ruppel, 2007, Mississippian Barnett Shale: Lithofacies and depositional setting of a deep-water shale-gas succession in the Fort Worth Basin, Texas: American Association of Petroleum Geologists Bulletin, v. 91, p. 579-601.
- Loutit, T. S., J. Hardenbol, P. R. Vail, and G. R. Baum, 1988, Condensed sections: The key to age determination and correlation of continental margin sequences, *in* C. W. Wilgus et al., eds., Sea Level Changes: An Integrated Approach: SEPM (Society for Sedimentary Geology) Special Publication 42, p. 183-213.
- Mapel, W. J., R. B. Johnson, G. O. Bachman, and K. L. Varnes, 1979, Southern midcontinent and southern Rocky Mountain region, *in* Craig, L. C., and C. W. Connor, coordinators, Paleotectonic Investigations of the Mississippian System in

- the United States, Part I: Introduction and Regional Analyses of the Mississippian System: United States Geological Survey Professional paper 1010—J, p. 161-187.
- Mitchum, R. M., P. R. Vail, and S. Thompson, III, 1977, The depositional sequence as a basic unit for stratigraphic analysis, *in* C. E. Payton, ed., *Seismic Stratigraphy—application to hydrocarbon exploration*: American Association of Petroleum Geologists Memoir 26, p. 53-62.
- Montgomery, S. L., D. M. Jarvie, K. A. Bowker, and R. M. Pollastro, 2005, Mississippian Barnett Shale, Fort Worth basin, north-central Texas: Gas-shale play with multi-trillion cubic foot potential: American Association of Petroleum Geologists Bulletin, v. 89, p. 155-175.
- Papazis, P. K., 2005, Petrographic characterization of the Barnett Shale, Fort Worth Basin, Texas: Master's thesis, University of Texas at Austin, Austin, Texas, 142 p., CD-ROM (SW0015), available from Bureau of Economic Geology, University of Texas at Austin.
- Passey, Q. R., S. Creaney, J. B. Kulla, F. J. Moretti, and J. D. Stroud, 1990, A practical model for organic richness from porosity and resistivity logs: American Association of Petroleum Geologists Bulletin, v. 74, p. 1777-1794.
- Plummer, F. B. and R. C. Moore, 1922, Stratigraphy of the Pennsylvanian formations of north-central Texas: University of Texas Bulletin, v. 2, 132 p.
- Pollastro, R. M., D. M. Jarvie, R. J. Hill and C. W. Adams, 2007, Geologic framework of the Mississippian Barnett Shale, Barnett-Paleozoic petroleum system, Bend arch—Fort Worth basin, Texas: American Association of Petroleum Geologists Bulletin, v. 91, p. 405-436.

- Posamentier, H. W., and G. P. Allen, 1999, Siliciclastic Sequence Stratigraphy—  
Concepts and Applications: SEPM (Society for Sedimentary Geology) Concepts  
in Sedimentology and Stratigraphy #7, 210 p.
- Ross, C. A., and J. R. P. Ross, 1987, Late Paleozoic sea levels and depositional  
sequences, in C. A. Ross and D. Haman, eds. Timing and deposition of eustatic  
sequences: Constraints on seismic stratigraphy: Cushman Foundation for  
Foraminiferal Research Special Publication 24, p. 137-149.
- Ross, C. A., and J. R. P. Ross, 1988, Late Paleozoic transgressive-regressive deposition,  
*in* C. W. Wilgus et al., eds., Sea Level Changes: An Integrated Approach: SEPM  
(Society for Sedimentary Geology) Special Publication 42, p. 227-247.
- Schmoker, J. W., 1981, Determination of organic-matter content of Appalachian  
Devonian shales from gamma-ray logs: American Association of Petroleum  
Geologists Bulletin, v. 65, p. 1285-1298.
- Supernaw, I. R., D. M. Arnold and A. J. Link, 1978, Method for in situ evaluation of the  
source rock potential of earth formations: United States Patent 4071755, 6 p.
- Vail, P. R., R. M. Mitchum, Jr., and S. Thompson, III, 1977, Seismic stratigraphy and  
global changes of sea level, Part 4: Global cycles of relative changes of sea level,  
*in* C. E. Payton, ed., Seismic Stratigraphy—application to hydrocarbon  
exploration: American Association of Petroleum Geologists Memoir 26, p. 83-97.
- Vail, P. R., F. Audemard, S. A. Bowman, Eisner, P. N., and C. Perez-Cruz, 1991, The  
stratigraphic signatures of tectonics, eustasy and sedimentology—an overview, in  
G. Einsele, W. Ricken, and A. Seilacher, eds., Cycles and Events in Stratigraphy:  
Berlin, Springer-Verlag, p. 617-659.

- Van Wagoner, J. C., H. W. Posamentier, R. M. Mitchum, P. R. Vail, J. F. Sarg, T. S. Loutit, and J. Hardenbol, 1988, An overview of sequence stratigraphy and key definitions, *in* C. W. Wilgus et al., eds., *Sea Level Changes: An Integrated Approach*: SEPM (Society for Sedimentary Geology) Special Publication 42, p. 39-45.
- Van Wagoner, J. C., R. M. Mitchum, K. M. Campion, and V. D. Rahmanian, 1990, *Siliciclastic Sequence Stratigraphy in Well Logs, Cores, and Outcrops*: American Association of Petroleum Geologists Methods in Exploration Series, No. 7, 55 p.
- Walker, R. G., 1992, Facies, facies models and modern stratigraphic concepts, *in* R. G. Walker and N. P. James, *Facies Models: Response to Sea Level Change*: Geological Association of Canada, p. 1-14.
- Walper, J. L., 1982, Plate tectonic evolution of the Fort Worth basin, *in* Martin, C. A., ed., *Petroleum Geology of the Fort Worth Basin and Bend Arch Area*: Dallas Geological Society, p. 237-251.



## APPENDIX 1

### List of Wells Used in This Study

Reference Number	Operator	Well Name
1	BRIDWELL OIL CO	BROWN LEWIS
2	BENNETT PROD CORP	AHRENS
3	WAGGONER W T EST	FULLER J B
4	TOLTEC OIL & GAS INC	WAGGONER
5	ENTERPRISE ENERGY	COLEMAN
6	DOUBLE EAGLE DRLG CO	FULGHAM W B 6
7	TAYLOR OPER CO	RUMAGE R O
8	H & S OPERATING INC	WATSON FELIX
9	TUTHILL & BARBEE	PATTERSON `A`
10	LANE OPERATING CO	GORDON
11	LANE OPERATING CO	GORDON
12	LANE OPERATING CO	SEIGLER
13	BURNS OPERATING LLC	LYNN BECKY
14	DALLAS PROD INC	PENNINGTON
15	Mitchell Energy	GRAHAM RANCH
16	Mitchell Energy	COLE TRUST ONE `A`
17	Mitchell Energy	SEALS G T
18	Mitchell Energy	KEELE KATHY
19	Mitchell Energy	COLE TRUST FOUR
20	Mitchell Energy	CALLAWAY P S GU
21	Mitchell Energy	COLE BOB
22	Mitchell Energy	COLE-LUKENS
23	ENRE L P MERIT ENERGY COMPANY	BLAIR HUNTER RANCH
24	REPUBLIC ENRGY INC	LEE LUTHER
25	REPUBLIC ENRGY INC	FLANAGAN
26	Devon	NELSON BYRON
27	J-W OPERATING CO	BLAIR
28	STAR OF TEXAS ENERGY	BUCHANAN
29	STAR OF TEXAS ENERGY	BUCHANAN
30	REPUBLIC ENRGY INC	LEE LUTHER
31	ENRE L P	MERRELL
32	J-W OPERATING CO	THOMPSON
33	STAR OF TEXAS ENERGY	NELSON-HYDE
34	STAR OF TEXAS ENERGY	NELSON-HYDE
35	REPUBLIC ENRGY INC	EWING GAIL
36	REPUBLIC ENRGY INC	SMITH

38	REPUBLIC ENRGY INC	TEXAS PROPERTIES
39	REPUBLIC ENRGY INC	LEE LUTHER
40	WINCHESTER PROD INC	SMITH
41	MEREKEN ENERGY CORP	OBENCHAIN
42	MEREKEN ENERGY CORP	OBENCHAIN
43	MEREKEN ENERGY CORP	OBENCHAIN
54	Mitchell Energy	LINDSEY RANCH
55	BEST PET EXPL INC	HESTER
56	CUMMING CO INC THE	WIMBERLY
57	3-R PRODUCTION INC	RUMAGE
58	3-R PRODUCTION INC	SPILLER
59	Four Sevens Operating	CRAFT J D
60	SWAN PRODUCTION CO	CHERRYHOMES MIKE
61	BEST PET EXPL INC	ANNA
62	SABRE OIL & GAS CORP	WEST LILLIE MAE
80	INDEPENDENT EXPL CO	STROUD J A
81	INDEPENDENT EXPL CO	JORDAN J B
82	STEPHENS HAYSEED OIL	MCCARTHY
83	DALLAS PROD INC	PEARSON WARREN
84	Mitchell Energy	GARRETSON T R
85	CUMMING CO INC THE	SMITH-ASHCROFT
86	3-R PRODUCTION INC	HUNT
87	ULTRA OIL & GAS INC	VAN ZANT
88	P L O INCORPORATED	ELDERS
89	DALLAS PROD INC	SUGGS
90	P-R-O MGMT INC	DYLAN
91	CROWN EQUIPMENT CO	PICKARD
92	CROWN EQUIPMENT CO	PICKARD
93	CHIEF OIL & GAS LLC	BEDINGER NORTH
94	ATOKA OPERATING INC	MCCLENDON ALMA
95	HARDING COMPANY	CAMPBELL-SUNDANCE-H
96	RANGE PRODUCTION CO	SEVEN KNOLLS
97	DTE GAS RESOURCS INC	CABANISS 259
98	ROWAN DRILLING CO	B L MARKUM
99	SOUTHEASTERN RES INC	EAGLE
100	ANADARKO	SANDSTROM `A`
101	AFE O&G CONSULT	GODFREY
102	AFE O&G CONSULT	COOK
103	CHIEF OIL & GAS LLC	SANDSTROM `A` UNIT
104	WALSH F H JR OPER CO	INDIAN CREEK
105	WALSH F H JR OPER CO	INDIAN CREEK
106	CHIEF OIL & GAS LLC	ELKINS UNIT
107	Devon	JOHNSON LOTTIE BART

108	WALSH F H JR OPER CO	INDIAN CREEK
109	WALSH F H JR OPER CO	INDIAN CREEK
110	Four Sevens Operating	BRUMBAUGH
111	MEEKER DAN MGNT INC	BAGBY
112	MEEKER DAN MGNT INC	RETTIG
113	CHIEF OIL&GAS COMPNY	GARNETT-LAPRELLE
114	WALSH F H JR OPER CO	INDIAN CREEK
115	Four Sevens Operating	GOLDEN TRIANGLE A
116	Four Sevens Operating	GOLDEN TRIANGLE I
117	CHIEF OIL & GAS LLC	ELKINS UNIT
118	Four Sevens Operating	E P R I
119	CH4 ENERGY CO LLC WESTERN PROD COMPANY	BELL
120	ANTERO RESOURCES INC	EAGLE VISTA
121	ANTERO RESOURCES INC	HAYCO
122	ANTERO RESOURCES INC	INDIAN CREEK
123	ANTERO RESOURCES INC	L&S LAND C
124	ANTERO RESOURCES INC	INDIAN CREEK
127	Mitchell Energy	CARTER A R
128	Mitchell Energy	ROHRER WILLIAM
129	Mitchell Energy	LAMANCE J W
130	Mitchell Energy	BUN JOHNSON UNIT
131	Mitchell Energy	YOUNG MARGARET
132	Mitchell Energy	WOMACK E A
133	Mitchell Energy	COLEMAN W S
134	Mitchell Energy	DONALDSON-WEBSTER
135	Mitchell Energy	ADAMS J S
136	Mitchell Energy	HOUGH H V
137	Mitchell Energy	PERKINS T W
138	Mitchell Energy	PAVILLARD ALBERT
139	Mitchell Energy	JESSIE SHIVE GAS UN
140	Mitchell Energy	FRANK J J GU `A`
141	MARCON OPER CO INC	KRAMER-NIVENS
142	Mitchell Energy	WISE JAMES E
143	Mitchell Energy	MCGEE THELMA
144	Mitchell Energy	PRUETT M E `A`
145	Mitchell Energy	WILLIAM TEDROW GAS
146	CHIEF OIL & GAS	NEIL AILEEN
147	Mitchell Energy	STELLA YOUNG GU `A`
148	Devon	MORRISON DEAN

149	Mitchell Energy	WISE JAMES E
150	UPHAM OIL & GAS CO	BARKSDALE ESTATE
151	MITCHELL ENRGY CO LP	MISS PAULINE
152	REPUBLIC ENRGY INC	SAUDER ALANE
153	MITCHELL ENRGY CO LP	TAYLOR CORA `A`
154	MITCHELL ENRGY CO LP	WAGGONER
155	UPHAM OIL & GAS CO	ORR WILLIAM
156	Devon	YOUNG STELLA GU
157	Devon	CURRIE FLORENCE
158	Devon	TEDROW WILLIAM GAS
159	Devon	WISE JAMES E GAS UN
160	Devon	SHEPHERD W J GAS UN

## APPENDIX II

### Elevation of Barnett Shale Flooding Surfaces

Ref.	GRS6	GRS5	Upper Forestburg Lime	Middle Forestburg	Lower Forestburg Lime	Lower Barnett
1	-5481	-5497				
2	-5265	-5288				
3	-5219	-5240				
4	-5254	-5278				
5	-5054	-5072				
6	-4721	-4738				
7	-5181	-5205				
8	-5397	-5421				
9	-5409	-5436				
10	-5103	-5129				
11	-5133	-5152				
12	-5110	-5127				
13	-4996	-5017				
14	-6833	-6848	-6869	-6907	-6979	-7041
15	-6597	-6634	-6643	-6679	-6759	-6829
16	-7110	-7145	-7196	-7248	-7282	-7338
17	-6981	-7015	-7057	-7083	-7141	-7218
18	-6869	-6902	-6937	-6971	-7053	-7094
19	-6976	-7011	-7054	-7100	-7152	-7233
20	-7016	-7051	-7099	-7129	-7205	-7291
21	-6928	-6962	-7006	-7026	-7098	-7190
22	-7116	-7152	-7200	-7224	-7306	-7402
23	-6831	-6870	-6926	-6955	-7019	-7084
24	-7101	-7138	-7185	-7202	-7288	-7371
25	-6737	-6781	-6822	-6850	-6881	-6900
26	-6906	-6942	-6986	-7012	-7097	-7184
27	-6731	-6776	-6814	-6841	-6874	-6898
28	-6866	-6905	-6959	-6994	-7052	-7117
29	-6734	-6773	-6822	-6853	-6914	-6944
30	-6733	-6775	-6821	-6848	-6906	-6935
31	-6748	-6789	-6836	-6865	-6918	-6938
32	-6810	-6847	-6893	-6923	-7002	-7059
33	-6822	-6860	-6908	-6936	-7013	-7087
34	-6787	-6827	-6878	-6912	-6964	-7007
35	-6791	-6830	-6883	-6912	-6970	-7003
36	-6840	-6879	-6934	-6964	-7016	-7075
37	-6826	-6868	-6918	-6949	-6998	-7027
38	-6732	-6775	-6817	-6848	-6879	-6909
39	-6751	-6794	-6838	-6864	-6894	-6914
40	-6867	-6903	-6945	-6975	-7025	-7065
41	-7015	-7055	-7112	-7148	-7198	-7243
42	-6903	-6942	-6997	-7031	-7087	-7160

43	-6924	-6963	-7018	-7056	-7105	-7179
54	-4771	-4801				
55	-3766	-3786				
56	-4688	-4705	-4723			-4731
57	-4891	-4899				
58	-4914	-4924				
59	-4948	-4978	-4986			-5136
60	-4849	-4859				
61	-4971	-4980				
62	-5144	-5161				
80	-4845	-4860				
81	-4424	-4430				
82	-4383	-4396				
83	-4319	-4345				
84	-5137	-5184				
85	-4433	-4483				
86	-4334	-4361				
87	-4547	-4563				
88	-5503	-5518				
89	-5412	-5420				
90	-4580	-4596				
91	-4945	-4955				
92	-4981	-4995				
93	-5108	-5130				
94	-4479	-4525				
95	-5614	-5633				
96	-5608	-5639				
97	-5008	-5045				
98	-5693	-5700				
99	-5947	-5977	-5990			-6031
100	-6007	-6052	-6057	-6063	-6069	-6071
101	-7245	-7254				
102	-6879	-6890				
103	-6057	-6101	-6109	-6116	-6123	-6126
104	-6065	-6108	-6118			-6125
105	-6079	-6119		-6133	-6136	-6141
106	-6077	-6118				-6136
107	-6346	-6383	-6401	-6417	-6424	-6433
108	-6019	-6054	-6066	-6070	-6080	-6084
109	-6021	-6054	-6066	-6071	-6081	-6091
110	-6334	-6374	-6393			-6399
111	-5968	-6003	-6007			-6012
112	-6358	-6397	-6400			-6404
113	-6342	-6384	-6398	-6402	-6404	-6407
114	-6113	-6143	-6158			-6203
115	-6382	-6422	-6436			-6440
116	-6359	-6400	-6406			-6412
117	-5999	-6042	-6050	-6057	-6061	-6065
118	-6337	-6377	-6395	-6403	-6410	-6413

119	-6877	-6889				
120	-6044	-6088	-6094			-6098
121	-6104	-6123				
122	-6002	-6033	-6046			-6090
123	-6040	-6059				
124	-6025	-6054	-6069			-6113
127	-5305	-5343	-5355	-5378	-5417	-5430
128	-5734	-5772	-5776	-5789	-5804	-5813
129	-5776	-5799	-5810	-5841	-5868	-5874
130	-5986	-6014	-6042	-6051	-6071	-6248
131	-5601	-5615	-5640	-5652	-5665	-5748
132	-5522	-5561	-5570	-5581	-5597	-5658
133	-5850	-5890	-5901	-5918	-5963	-6052
134	-5197	-5243	-5245	-5249	-5259	-5265
135	-5650	-5693	-5703	-5710	-5738	-5743
136	-5944	-5976	-5988	-6007	-6027	-6189
137	-5825	-5852	-5863	-5881	-5897	-6036
138	-5947	-5967	-5984	-5994	-6020	-6123
139	-5866	-5894	-5912	-5925	-5940	-6085
140	-6147	-6172	-6178	-6217	-6271	-6291
141	-5388	-5409	-5425			-5603
142	-5869	-5892	-5913	-5922	-5939	-6053
143	-6398	-6436	-6449	-6454	-6470	-6673
144	-5368	-5404	-5411	-5413	-5425	-5437
145	-6090	-6111	-6125	-6147	-6201	-6233
146	-6019	-6051	-6071	-6081	-6102	-6267
147	-5877	-5906	-5916	-5935	-5952	-6110
148	-5946	-5967	-5997	-6032	-6047	-6239
149	-5883	-5906	-5920	-5936	-5957	-6074
150	-5706	-5726	-5754	-5770	-5813	-5922
151	-6539	-6573	-6592	-6600	-6616	-6796
152	-6227	-6248	-6269	-6275	-6298	-6522
153	-6440	-6466	-6494	-6499	-6514	-6679
154	-6353	-6371	-6405	-6413	-6427	-6632
155	-5526	-5544	-5575	-5585	-5648	-5741
156	-5887	-5912	-5932	-5942	-5960	-6086
157	-6108	-6128	-6138	-6150	-6212	-6284
158	-6121	-6141	-6155	-6181	-6233	-6267
159	-6043	-6066	-6087	-6097	-6117	-6234
160	-5971	-5985	-6015	-6022	-6044	-6143

	GRS4	GRS3	GRS2	GRS1	Base
1	-5519				
2	-5309	-5388	-5470	-5485	-5492
3	-5260	-5344	-5413	-5435	-5441
4	-5301	-5374	-5435	-5459	-5467
5	-5094	-5171	-5220	-5240	-5243
6	-4756	-4827	-4875	-4898	-4899
7	-5225	-5317	-5382	-5403	-5404

8	-5448	-5537	-5641	-5665	-5667
9	-5462	-5558	-5626	-5637	-5643
10	-5151	-5247	-5305	-5338	
11	-5172	-5264	-5310	-5325	-5327
12	-5146	-5238	-5295		-5323
13	-5029	-5125	-5173	-5199	-5204
14	-7096	-7234	-7343	-7372	-7375
15	-6877	-7003	-7110	-7140	-7141
16	-7396	-7692	-7833	-7866	-7868
17	-7276	-7460	-7580	-7613	-7614
18	-7193	-7376	-7493	-7517	-7519
19	-7295	-7535	-7667	-7700	-7701
20	-7343	-7506	-7629		
21	-7237	-7407	-7531	-7569	-7570
22	-7443	-7620	-7745	-7787	-7788
23	-7125	-7272	-7389	-7429	-7430
24	-7420	-7614	-7742	-7777	-7779
25	-6936	-7066	-7170	-7200	-7202
26	-7229	-7389	-7508	-7548	-7549
27	-6910	-7044	-7144	-7174	-7177
28	-7159	-7302	-7415	-7449	-7453
29	-6973	-7107	-7215		
30	-6965	-7102	-7206		
31	-6968	-7104	-7208	-7237	-7239
32	-7124	-7273	-7386	-7424	-7426
33	-7127	-7273	-7389	-7426	-7428
34	-7040	-7180			
35	-7038	-7177			
36	-7112	-7254	-7367	-7399	-7404
37	-7050	-7190	-7298	-7329	-7334
38	-6935	-7069			
39	-6951	-7082			
40	-7098	-7238	-7348	-7379	-7381
41	-7326	-7480	-7602	-7640	-7647
42	-7203	-7353	-7468	-7501	-7508
43	-7222	-7369	-7481	-7517	-7520
54					
55	-3798				
56	-4758	-4810	-4913	-4945	-4946
57	-4932	-5006	-5077	-5106	-5110
58	-4955	-5024	-5096	-5126	-5127
59	-5159	-5306	-5454	-5487	-5487
60	-4883	-4959	-5043		-5073
61	-5004				
62					
80	-4868	-4945	-5020		
81	-4444	-4523	-4581	-4641	-4646
82	-4407	-4472	-4533	-4579	-4583
83	-4376	-4444	-4510	-4543	-4545



84	-5202	-5271	-5345	-5390	-5393
85	-4495	-4556	-4623	-4653	-4655
86	-4394	-4472			
87	-4603	-4679			
88	-5531				
89	-5442	-5519			
90	-4606	-4692			
91	-4965	-5043	-5108	-5146	-5149
92	-5012	-5119			
93	-5138	-5230	-5290	-5342	-5344
94	-4549	-4606	-4670	-4707	-4710
95	-5646	-5756	-5817	-5884	-5888
96	-5656	-5754	-5829	-5899	-5905
97	-5069	-5149	-5228	-5309	-5312
98	-5717	-5832	-5941	-6047	-6048
99	-6052	-6148	-6236	-6286	-6301
100	-6080	-6185	-6268	-6316	-6332
101	-7272	-7384	-7493	-7615	-7632
102	-6909	-7040	-7151	-7240	-7241
103	-6133	-6239	-6324	-6372	-6389
104	-6142	-6248	-6333	-6382	-6401
105	-6158	-6261	-6347	-6396	-6412
106	-6155	-6258	-6342		
107	-6440	-6554	-6639	-6676	-6680
108	-6101	-6202	-6284	-6330	-6344
109	-6111	-6213	-6289	-6336	-6349
110	-6421	-6539	-6623	-6656	-6658
111	-6028	-6143	-6213	-6267	-6277
112	-6421	-6547	-6620		
113	-6429	-6545	-6631	-6667	-6674
114	-6227	-6329	-6417	-6462	-6465
115	-6459	-6581	-6667	-6702	-6703
116	-6430	-6554	-6628	-6670	-6681
117	-6073	-6176	-6260	-6307	-6331
118	-6427	-6544	-6631	-6661	-6664
119	-6908	-7020	-7120	-7232	-7249
120	-6116	-6220	-6302	-6348	-6365
121	-6137	-6275	-6354	-6416	-6426
122	-6113	-6212	-6294	-6345	-6357
123	-6074	-6211	-6291	-6327	-6331
124	-6137	-6238	-6324	-6371	-6374
127	-5457	-5536	-5680	-5748	-5750
128	-5831	-5903	-6017	-6069	-6069
129	-5893	-5972	-6086	-6133	-6134
130	-6278	-6432	-6542	-6575	-6575
131	-5777	-5854	-5951	-5986	-5988
132	-5681	-5760	-5906	-5986	-5986
133	-6075	-6170	-6278	-6315	-6315
134	-5279	-5345	-5446	-5482	-5492

135	-5766	-5839	-5963	-6027	-6029
136	-6231	-6328	-6430	-6472	-6474
137	-6070	-6161	-6245	-6272	-6274
138	-6153	-6241	-6342		
139	-6120	-6211	-6313	-6351	-6353
140	-6317	-6412	-6514	-6558	-6559
141	-5630	-5884	-5996	-6049	-6050
142	-6083	-6173	-6274	-6311	-6313
143	-6724	-6825	-6928	-6966	-6968
144	-5469	-5537	-5650	-5724	-5742
145	-6262	-6359	-6459	-6497	-6498
146	-6307	-6406	-6503	-6543	-6544
147	-6137	-6230	-6331	-6375	-6376
148	-6253	-6400	-6501		
149	-6103	-6193	-6295		
150	-5957	-6055	-6189	-6236	-6237
151	-6875	-6983	-7088	-7124	-7125
152	-6545	-6736	-6841	-6888	-6893
153	-6776	-6913	-7021	-7063	-7065
154	-6686	-6881	-7000	-7038	-7038
155	-5777	-5855	-5990	-6059	-6060
156	-6122	-6213	-6315	-6355	-6356
157	-6311	-6407	-6505	-6547	-6548
158	-6296	-6392	-6494	-6533	-6534
159	-6266	-6355	-6455	-6495	-6496
160	-6172	-6260	-6362	-6401	-6402

## APPENDIX III

### Isopach Values of Units within Barnett Shale

Reference	Barnett Thickness (Feet)	GRS 6-5	Forestburg Lime Thickness	Middle Forestburg Shale Thickness	Lower Barnett- GRS 4
1		16			
2	228	23			
3	223	21			
4	212	24			
5	190	18			
6	178	17			
7	223	24			
8	270	24			
9	234	27			
10	257	26			
11	194	19			
12	214	18			
13	208	20			
14	542	15	172	72	55
15	543	38	186	80	49
16	757	35	142	33	58
17	633	35	161	57	58
18	650	33	157	82	99
19	725	35	178	52	62
20		36	192	76	51
21	642	35	184	73	47
22	672	36	201	82	41
23	599	39	158	64	41
24	677	36	185	86	49
25	465	44	79	31	35
26	643	36	199	85	44
27	443	44	84	33	12
28	587	39	158	58	42
29		39	122	61	30
30		41	114	58	30
31	491	41	102	53	30
32	616	37	166	78	42
33	606	38	179	76	40
34		39	129	53	33
35		39	120	58	35
36	561	39	141	53	37
37	508	42	109	49	23
38		43	92	31	26
39		43	76	30	37
40	514	36	119	50	33
41	632	40	132	50	83
42	605	39	164	55	42
43	597	39	162	50	43
54		30			

55		20			
56	258	17	8		27
57	219	9			
58	212	10			
59	539	30	150		23
60	224	10			
61		9			
62		17			
80		15			
81	223	6			
82	200	13			
83	227	27			
84	257	47			
85	222	49			
86		27			
87		17			
88		15			
89		8			
90		16			
91	204	9			
92		15			
93	236	22			
94	231	45			
95	274	19			
96	292	31			
97	304	36			
98	355	7			
99	354	30	41		21
100	325	45	14	6	9
101	387	9			
102	363	11			
103	331	43	17	7	7
104	336	43	7		18
105	333	40		3	17
106		41			19
107	334	37	32	7	7
108	324	34	18	10	18
109	328	33	25	11	20
110	324	40	7		22
111	308	37	4		
112		39	5		16
113	332	42	9	2	22
114	352	31	45		24
115	322	42	4		19
116	322	41	6		18
117	332	44	15	4	8
118	327	40	18	8	13
119	372	12			
120	321	43	4		18
121	323	20			
122	355	32	44		22
123	291	19			
124	349	29	44		24
127	444	38	76	39	27

128	335	38	37	15	18
129	358	22	64	27	19
130	589	29	206	19	30
131	386	13	108	19	29
132	464	39	88	17	23
133	465	39	151	45	23
134	294	45	20	10	
135	376	43	40	27	23
136	531	32	201	20	41
137	449	27	173	16	34
138		20	139	27	30
139	486	27	173	16	35
140	412	25	113	54	27
141	662	21	178		26
142	443	23	139	17	30
143	570	38	224	17	51
144	374	36	26	12	32
145	408	20	108	54	29
146	525	32	196	21	40
147	499	29	194	16	27
148		21	242	15	14
149		23	154	21	29
150	531	21	168	43	35
151	587	34	204	16	78
152	666	20	253	23	23
153	625	27	185	14	97
154	685	18	227	14	54
155	534	18	166	63	36
156	469	25	154	18	35
157	440	20	146	62	27
158	413	20	112	52	29
159	453	23	147	20	32
160	431	14	127	22	30

Reference	GRS 5-4	GRS 4-3	GRS 3-2	GRS 2-1	GRS 1- Barnett Base
1	22				
2	21	79	82		7
3	20	84	69		6
4	24	73	61	24	7
5	22	76	49		3
6	18	70	48	23	2
7	19	92	64		1
8	26	89	104	24	2
9	26	96	68		6
10	22	97	58	33	
11	20	92	46		2
12	19	92	57		
13	12	96	47	26	5
14	248	139	109	28	4
15	243	125	106	31	0
16	251	296	141	33	2
17	261	184	120	33	1
18	291	183	117	24	2

19	284	241	132	33	1
20	291	164	123		
21	275	170	124	38	1
22	291	177	125	41	1
23	256	147	116	40	2
24	282	194	129	35	2
25	155	130	104	30	2
26	287	160	119	40	1
27	134	134	100	30	1
28	254	143	113	34	3
29	200	133	109		
30	190	137	104		
31	179	136	104	28	3
32	277	149	113	38	2
33	267	146	117	37	2
34	213	140			
35	207	139			
36	233	142	114	31	2
37	182	140	109	30	5
38	160	134			
39	157	131			
40	195	141	110	31	2
41	271	155	122	38	7
42	261	150	116	33	6
43	259	147	112	36	3
54					
55	12				
56	53	52	103	32	1
57	32	75	71	29	4
58	31	69	71	30	1
59	181	147	148	32	1
60	25	76	84		
61	24				
62					
80	8	76	76		
81	15	79	58	59	6
82	11	66	61	46	3
83	31	68	66	33	3
84	18	69	74	45	3
85	12	60	67	30	2
86	33	77			
87	39	76			
88	13				
89	23	77			
90	10	86			
91	10	79	64	38	3
92	16	108			
93	8	92	60	52	2
94	24	57	64	37	4
95	13	109	61	67	4
96	16	99	73	71	6
97	25	79	79	81	3
98	15	117	109	105	2
99	75	96	88	50	15

100	28	105	83	48	17
101	18	112	109	122	17
102	20	131	111	88	2
103	32	106	86	48	16
104	34	106	86	49	19
105	39	103	86	49	16
106	37	103	84		
107	57	114	85	37	4
108	48	100	82	46	14
109	58	101	77	47	13
110	47	118	84	33	2
111	24	115	71	53	8
112	24	126	73		
113	46	116	86	36	6
114	83	103	87	45	3
115	36	122	86	36	0
116	30	124	74	41	12
117	31	103	84	47	24
118	50	117	87	31	2
119	18	112	100	112	17
120	29	103	83	45	18
121	14	138	79	62	10
122	79	100	82	51	11
123	15	137	80	36	4
124	83	101	86	47	2
127	114	78	144	68	1
128	59	72	114	52	0
129	94	79	114	47	1
130	264	154	109	33	0
131	162	77	96	36	1
132	120	79	146	80	0
133	186	95	108	36	0
134	36	67	100	36	10
135	73	73	124	64	0
136	255	97	102	42	3
137	219	91	84	27	2
138	186	88	101		
139	226	91	102	38	2
140	145	94	103	44	1
141	221	255	111	53	1
142	191	90	101	37	1
143	288	100	104	38	2
144	65	68	113	74	17
145	151	97	100	38	1
146	257	99	98	39	1
147	231	93	102	44	1
148	286	147	102		
149	197	91	101		
150	231	98	133	47	1
151	302	108	105	37	1
152	297	192	104	48	4
153	310	136	108	42	2
154	315	195	119	38	0
155	233	78	135	69	1

156	210	92	102	40	1
157	183	96	98	43	0
158	155	96	102	39	1
159	200	89	100	39	1
160	188	87	102	39	1



## VITA

### Personal Background

Michael Bailey Steed  
Fort Worth, Texas  
Born May 16, 1983, Dallas, Texas  
Son of Jerry and Barbara Steed

### Education

Bachelor of Science  
Environmental Earth Resources, 2006  
Texas Christian University, Fort Worth, TX

Master of Science in Geology, 2009  
Texas Christian University, Fort Worth, TX

### Experience

Teaching Assistant, 2006-2008  
Texas Christian University, Fort Worth, TX

Intern Geologist, 2006-2008  
Jetta Operating Inc., Fort Worth, TX

### Professional Memberships

Fort Worth Geological Society (FWGS)  
Houston Geological Society (HGS)  
American Association of Petroleum Geologists (AAPG)

## **ABSTRACT**

Sequence Stratigraphy of the Barnett Shale  
(Mississippian), northern Fort Worth basin, Texas

By Michael B. Steed, M.S., 2009  
Department of Geology  
Texas Christian University

Thesis Advisor: Dr. John Breyer, Professor of Geology

The Barnett Shale was deposited in a deep, anoxic, basin during the Mississippian. High amounts of organic matter were preserved under the prevailing anoxic conditions along with fine-grained pelagic and hemipelagic sediment. The sediment was deposited in a foreland basin on the southern edge of the North American craton during a prolonged second-order highstand of sea level. Sediment was also introduced into the basin by turbidity currents and debris flows from surrounding shelfal environments. During the deposition of the Barnett Shale, sea level fluctuated many times, and during highstands of sea level, condensed sections formed in basinal settings. Condensed representing maximum flooding surfaces can be correlated across the Fort Worth basin using gamma ray logs.